TREATISE ON GEOCHEMISTRY

SECOND EDITION

VOLUME 1-16

H.D. Holland Executive Editors K.K. Turekian

13.4 Dating and Tracing the History of Ore Formation

HJ Stein, Colorado State University, Fort Collins, CO, USA; University of Oslo, Oslo, Norway

Tribute to Dick Holland – About ten years ago I received a phone call and a gentle but deliberate voice said 'I heard you can date pyrite.' It was Dick Holland cautiously jazzed about the possibility that we might be able to precisely date diagenetic pyrite in Paleoproterozoic shale at Timeball Hill, South Africa. I laughed. It worked. And the first absolute time pin for the rise of atmospheric oxygen was established resulting in two publications with Dick (Bekker et al., 2004; Hannah et al., 2004a). So clever he was. Dick first opened my eyes to the treasure trove of science in black shales. – HJS

13.4.1   A Holistic Approach to Ore Geology

Economic geologists study ore deposits. Two pieces of information are critical for their study – the timing of ore deposition and source rock. The compositions of ore-forming fluids, whether measured from fluid inclusions or estimated from ore minerals, are used to back our way into the question of source rock. But in reality, these data are merely in situ end measurements based on long and arduous journeys of fluids in the crust. Timing of ore deposition has been tackled through traditional U–Pb and ^{40}Ar–^{39}Ar dating of minerals associated with magmatic–hydrothermal processes, and more recently with Re–Os geochronology where the sulfides themselves are directly dated. In addition, Re–Os offers a tracer isotopic ratio, ^{187}Os/^{188}Os, that provides information on the ore fluid source and/or its history. Timing and source are the pieces that allow us to move from description to interpretation at a scale beyond deposit, district, and mineral belt, and allow us to decipher the processes that move and distribute material among Earth reservoirs (Figure 1).

Breakthroughs and new understanding of ore deposits have come largely from outside the traditional discipline of economic geology. Most traditional economic geology literature concludes simply that ore fluids are either mantle-derived or crustally derived based on tallies of isotopic or other geochemical data at the deposit scale. But the many processes that move metals from their true source through the crust to a welcoming locality for ore deposition are not easily accessed by our data assemblies. A better understanding of those processes will improve our identification of source rocks. In the next decade, skill sets that account holistically for downward metal transport from aerosols to photic zone to seabed, balanced by cycling of metals from crust to mantle and mantle to crust, will be in demand.

Dynamic plate reconstructions pinned to absolute time based on direct dating of sulfide are essential to understanding metallic resources. And conversely, reconstructions must be informed by the many well-organized reserves of descriptive information that exist for ore deposits. Rather than geographically outlining mineral belts, it is essential to place craton, subcraton, and craton–margin processes on reconstructed paleocontinents to interpret the metallogenic past. Many compilations of metallogenesis through time are based on amassed literature age data without informed understanding of quality, context, and technique employed. These compilations are often carried out by those without any expertise in geochronology. This approach can lead us astray. Meaningful geochronology requires ages for samples placed in well-constrained spatial and paragenetic contexts. We now have the technology to build real time bins for metallogenic processes from hard isotopic data acquired directly from the ore minerals. To bring ore geology to a new level of enlightenment requires that economic geologists merge their expertise with workers from diverse fields, from mantle dynamics to isotope geochemistry. To understand ore deposits, we need to understand metal mobility through time in a three-dimensional (3D) whole-Earth perspective.

This book is specific to mineral resources. Therefore, the emerging field of Re–Os isotope geochemistry that enables direct dating of ore minerals is emphasized. The details and systematics for other traditional dating methods can be found in textbooks and in the literature. Re–Os dating of sulfides and oxides is used to illuminate the fundamentals of radioisotope geochronology. This chapter presents issues tackled to bring Re–Os dating into the field of economic geology and, in turn, shows how sulfide chronology has begun to contribute to disciplines external to economic geology. Real examples are used as illustrative material. These examples will assist the economic geologists without a background in geochronology to work more knowledgably and effectively with age information.

Finally, many of the articles cited in this chapter were selected, in part, because they fall outside the cycle of literature quoted in traditional economic geology journals. The aim is to draw attention to highly relevant literature in ancillary disciplines – literature that offers much toward understanding ore genesis. This provides a holistic foundation for understanding fluids in the crust and their journey toward ore formation.

Figure 1   The three primary reservoirs for metals in Earth's crust and fundamental Earth processes impacting metal budgets through time. Fluids in the crust are simultaneous carriers of soluble metals and variable amounts of hydrocarbon. Source rocks, anything from metalliferous shales to gneissic rocks, are parental material for fluid and migrated metals. Receipt and release of metals in the mantle provide dynamic oversight at the global scale.

13.4.1.1   What We Know

We know very little about Earth as a whole, though we are marvelous describers and recorders of our observations. Interpretation based on our senses is easy, but interpreting out-of-sight processes in the lithosphere operating on geologic time frames takes far more imagination. We rely on 3D exposures of high mountain localities and tiny strings of information

recovered from drill holes that are strongly concentrated where resources have been discovered or are probable. The global drill hole record, skewed toward resource-rich regions, gives us more familiarity with the anomalies than the average rock.

Our observational, descriptive and classification skills are nowhere better honed than at the scale of the ore deposit. Since the field of economic geology came into being more than 100 years ago, we have unwaveringly performed the task of constructing 3D models of ore deposits and assigning relative time relationships to sort out the ore-forming history. We have faithfully recorded vein widths, morphologies, mineralogies, orientations, alteration envelopes, and cross-cutting relationships in great detail – through drill core and underground and open pit mapping. With the rock and ore record at the deposit scale we have produced colorful rotating graphics allowing us to view the prize from virtually any perspective. We are good at visually organizing events in space. But, as recently as 1996, 'dating of a single ore mineral has not yet been successful' (Frei and Pettke, 1996), though pioneering attempts to directly date molybdenite and pyrite had been made (Herr and Merz, 1955; York et al., 1982).

13.4.1.2   Critical and Compromising Gaps

Our descriptive approach to ore geology has served us well but lacks a fundamentally important element – TIME. While cross-cutting relationships accurately record *relative* time, the actual time elapsed between two events cannot be known without direct dating of a robust mineral phase firmly attached to each event. Without some sense of *absolute* time, our understanding of scale and scope of processes involved is compromised.

A common misperception in economic geology is that the ore-forming process can be reduced to a single crescendo of events that ultimately constructs an ore deposit, and that this same symphonic sequence is episodically played through geologic time and across geographic space. As an example, the globally employed concept of an ore-forming volcano–plutonic complex has netted us the model of vein sets and vein types, followed by more subtypes that we attribute to unique singular positions in the paragenesis – and in time (e.g., Cannell et al., 2005; Gustavson and Hunt, 1975; Sillitoe, 2010). Re–Os dating, however, shows that individual vein-forming events and local cross-cutting relationships from *different parts* of the magmatic–hydrothermal environment may not correlate in time. Re–Os dating in the volcano–plutonic environment allows deconstruction of ore formation on a vein-by-vein basis. The time component is revising long-held ore deposit models and yields a more realistic conceptual framework for ore-forming processes in a heterogenous earth.

In reality, the ore-forming environment is one of chemical and physical chaos and disequilibrium from the nanometer to the multikilometer scale. Hundreds of microscale measurements acquired from small volumes of rock in very large systems may not be our best tool to characterize and categorize ore deposits. Similarly, sweeping generalities driven by the need to pidgeonhole a deposit as belonging to a certain type disables the imagination. These compromising gaps require use of the only sure correlation tool to bridge issues of scale – absolute time.

In Section 13.4.5.4, the noncontemporaneity of vein types traditionally used to correlate time in the porphyry environment is demonstrated in the context of a tutorial on how to examine a Re–Os data set for generations of molybdenite deposition.

13.4.1.3   Meaningful Results

Given our working media is completely inhomogeneous and largely in disequilibrium, how do we go about acquiring meaningful geochronologic results? There are four critical steps *prior to* analytical work leading to radiometric age data.

First, formulation of a clear question is a prerequisite to collecting samples. Samples should be acquired based on their geologic relevance to the question. The 'do the isotopes' approach as part of an information package for 'the geology and origin of the ore deposit' is not particularly thoughtful. Geochronologic data are generally derived from a single mineral phase (or group of phases), and hence, the age information applies only to the isotopic integrity of that phase (see Section 13.3.2.3). The data are of minimal use for ore geology unless the paragenesis of dated phase is well known in relative time and space.

Second, the assumptions and statistical manipulation of isotopic data are minimally understood by most users of the data. Economic geologists with lab experience or in-depth understanding in isotope geology are, in fact, exceedingly rare. To assure that requesters and generators of isotopic data create comprehensive and credible results that are put to full use, geologist and geochronologist must work hand-in-glove from the start.

Third, it is easy to be unduly distracted by precision. High precision does not affirm accuracy. The statistical acquisition and meaning of uncertainty for an isotopic age varies with different isotopic systems. Within a given system, the reported '±' uncertainty depends strongly on data reduction protocols. In all cases, however, the uncertainty is analytical, and tells little about the true accuracy of an age. As well stated by a mathematician, 'it is better to be approximately correct than precisely wrong' (Tukey, 1962).

Fourth, meaningful science derives from understanding process, not myopic examination and isolation of singular events. The formation of ore deposits, like all other geologic processes, is the consequence of multiple events spread through geologic time. Just as the rests in music are as essential as the notes played, the time between events is well worth understanding to put the whole of the process together. What halts an event, and what restarts the process? Our estimates of ore-forming processes and their composing events via geochronology give us parameters to work with, not within. There is no reason to expect, for example, that all porphyry deposits should require >2 million years to form (e.g., Sillitoe and Mortensen, 2010), or <1 million years to form (e.g., von Quadt et al., 2011). One estimate of 55 000 years for construction of an epithermal Au deposit in Papua New Guinea is based on a measured present-day Au flux in an active volcanic system (Simmons and Brown, 2006); it is difficult to imagine an unchanging rate of discharge and/or Au content in a fluid over tens of thousands of years – particularly as significant changes in fluid discharge and composition are routinely

measured today during volcanic monitoring. In addition, merging results from field measurements and geochronology with theoretical modeling (e.g., Cathles and Shannon, 2007; Cathles et al., 1997) presents an even greater challenge. The ongoing duration debate in recent literature distracts us from the real issue at hand, that is, the source and mobility of metals within and entering the crust and the larger timescales for enrichment.

13.4.1.4   Meaningful Models

Models are the invention of imagination, and they both stimulate and limit creativity. Since models are limited by visual access to spatial connectivity, absolute time has a critical role to play for correlation. In recent years, new technology and new machinery has enabled rapid collection of vast sums of geochemical measurements on very small samples (e.g., fluid inclusions and minerals at the microscale). If many of these geochemical data sets are tallied from environments characterized by disequilibrium, how can we best merge these data with larger scale observational data to better understanding how ore deposits are assembled? The long-held concept of ore deposit models has long provided a rudimentary basis for comparing data and observations between different ore deposit types. But this is not without challenge.

The classification and categorization of ore deposits has changed remarkably little in the last 100 years. Pioneering work by Emmons (1904) solidified the concentric correlation between ore and unseen intrusive rocks through radiating patterns of dikes. Still today, a first response is to relate many ore types to an intrusion, seen or unseen. Renowned ore geologist Graton (1941) wrote in his 50-year retrospective of the field of ore deposits 'The profound importance of these space–time-genesis relationships in putting a new quality of order, consistency, and meaning into virtually the entire range of ore deposition cannot be overemphasized.' Yet, order is assigned by grouping mineralogical similarities and familiar ore geometries to advance 'ore deposit models.' In fact, this concept has partly sidelined economic geology and limited exchange with other geoscience disciplines. An example of model failure in the last twenty years is the creation of a new model to house a diverse class of ore deposits called IOCG (iron oxide copper gold; e.g., Barton, **Chapter 13.20**; Groves et al., 2010). Among other parameters, radiometric dating of IOCG deposits has turned in ore formation ages spanning hundreds of thousands to hundreds of millions of years. There is no unifying geometry or genesis for this rag–tag grouping, leading to frequent literature labels such as 'a variation of the IOCG.' When too many members of a population become the exceptions, this is a clear signal that the imposed classification scheme is flawed. The same classification pitfalls apply to models for orogenic gold deposits. Geochronology is essential to correctly link ore deposition with geologic processes in time and space. Models without Graton's 'time–space-genesis' connection provide only soft generalities, not specific guides to understanding.

Still today, economic geologists use the terminology epithermal, mesothermal, and hypothermal to describe ore deposits relative to their presumed depth of emplacement based primarily on temperature associated with ore deposition (Lindgren, 1933). While this concept is a useful starting point,

geologic processes traverse vast vertical depths and penetrate lateral dimensions; thus, a complex magmatic–tectonic system may generate ore deposits at several levels. For example, in the last 20 years, our understanding of how plutons and stocks are constructed has changed profoundly (e.g., Paterson et al., 2011; Schmitt et al., 2003). Cooling of an ore-related stock is no longer a calculation based on a static and singular cooling event following emplacement of melt into shallow crust. Rather, the process is one of dynamic upheaval, exchange and assimilation, and timescales vary relative to local conditions regardless of position in the crust. Stoping and assimilation are two slippery variables (Beard et al., 2005; Glazner, 2007) – their very concept confronts underlying assumptions of isotopic equilibrium in magma chambers (Beard, 2008). If the starting parameter for a magmatic-related ore deposit (intrusive to metamorphic) is a system in isotopic disarray, it is clear that isotopic measurements on smaller volumes of once-removed generations of sulfides from that system will be further complicated. To meet the resource needs of the twenty-first century head on, models that have remained nearly unchanged for too long need to be reexamined. Geochronologists provide data critical to this task, provided thoughtful sampling is undertaken to capture and correlate discrete increments of time. This requires that geochronologists work closely with knowledgable geologists on site.

13.4.2   The Fourth Dimension – Time

The concept of time for physicists differs significantly from that of geologists. This leads to probing questions about the long-term constancy of decay constants used in chronology. At the scale of geologic time, radiometric decay constants are generally treated as constant. This provides the basis to broadly relate and correlate geologic processes at the global scale. Consistency in age results utilizing different geochronometers verifies this simplistic first-order assumption at geologic timescales. With increasingly precise technologies, however, small inconsistencies in long-standing assumptions are revealed (e.g., Hiess et al., 2012). Thus far, most small inconsistencies are overwhelmed by the geologic uncertainty imposed by heterogeneous Earth processes. Still, future improvements in geochronology depend on continued assessment and revision of decay constants (e.g., Rotenberg et al., 2012).

13.4.2.1   The Transcendence of Time

There is only one dimension in geology that quantifies rates and permits absolute correlation of processes and events on disparate continents and across both past and present oceans, and that dimension is geologic time. We use geologic time to organize past events and to predict the future. Without radiometric clocks in Earth materials, our correlative ability draws on identification of like features, sequences and patterns, and faunal appearances and disappearances. We are easily led to assign time relationships without absolute time. But this action assumes we know rates and that those rates are constant. In fact, we do not know past rates, and our observations today tell us that rates for Earth processes are not constant. Cross-cutting relationships and biostratigraphy provide us with indisputable

relative time relationships, but they tell us nothing of absolute time. Absolute time transcends lithology and biota, and all aspects of Earth systems. A package of ten magnetic reversals (chrons) occurring in ten million years does not give us license to assume that each chron lasted for one million years. Ten meters of black shale deposited over ten million years does not support the practice of dividing by ten to assume that one meter of shale is deposited every one million years.

So, too, is this the situation for ore geology. The time interval between two cross-cutting veins at one locality cannot be transferred wholesale to another geographically separated vein set in the same deposit, much as they may appear alike. Multiple ore-filled breccia pipes or collapse structures collectively constituting an ore deposit do not all form at the same time.

13.4.2.2 Time Ties that Bind

In complex environments where metals are on-the-move in Earth's crust, we need secure radiometric clocks that are either impermeable or fully respond to the passage of later fluids. They must either reject or fully accept subsequent heating and deformation. Fully retentive or fully responsive clocks provide time ties that bind. A partial response may be difficult to recognize and interpret.

13.4.3 Radiometric Clocks

All radiometric clocks operate on the same basic principle: a radioactive 'parent' isotope of one element decays to a stable 'daughter' isotope of another element at a constant rate on geologic timescales. The parent–daughter transformation may occur in a single step, or it may involve the formation of many intermediate decay products before reaching the stable daughter isotope. To be useful, the half-life of the parent isotope, the time it takes to decay half of the initial quantity of parent, must be on the same order of magnitude as the time span to be measured. That is, ages for Holocene events are best determined using short-lived isotopes, whereas events 10^8 or 10^9 years in the past require isotopes with half-lives on par with the age of the earth. In this way, there is ample parent remaining to measure and time for measurable daughter to accumulate. The rate of decay is expressed as the decay constant. The half-life ($t_{1/2}$) and decay constant, lambda (λ), are mathematically related ($t_{1/2} = \ln 2/\lambda$).

The most widely used chronometers in economic geology are ^{187}Re–^{187}Os, ^{235}U–^{207}Pb, ^{238}U–^{206}Pb, ^{87}Rb–^{87}Sr, ^{147}Sm–^{143}Nd, and $^{40}Ar/^{39}Ar$ (related to parent ^{40}K and irradiation of ^{39}K to produce ^{39}Ar). Each chronometer has unique strengths and limitations; the key is to know which chronometer best addresses the question at hand. A text book in isotope geology (e.g., Faure and Mensing, 2005) provides the fundamentals for these different dating systems.

13.4.3.1 What Geologic Clocks Measure

The coveted time pieces in geochronology applied to ore deposits have traditionally been the clocks that retain primary ages. Primary ages generally refer to depositional ages in the

sedimentary environment and volcano–plutonic ages in the magmatic environment. Metamorphism and hydrothermal alteration are by definition secondary events, as original rocks are changed by both new temperature–pressure conditions and metasomatism. If secondary events are close in time to primary ages, the geologic clock may be imperceptibly disturbed or a small amount of noise (uncertainty) may be introduced into a still meaningful age result. The longer the time gaps between primary and secondary events, the more significant the potential isotopic disturbance. For any chronometer, even a miniscule loss or gain of parent or daughter in the recent past (e.g., weathering) has huge impact on the geochronology.

Commonly, the unique concepts of isotopic disturbance versus isotopic resetting are erroneously used interchangeably as explanations for isotopic data sets. Disturbance refers to incomplete isotopic exchange, whereas resetting refers to perfect isotopic homogenization following a disturbance event (Figure 2). True primary ages and fully reset ages are reproducible among like samples and certainly within samples. In contrast, isotopic disturbance is highly unlikely to be identically reproducible among and within samples, because the process is partial and incomplete, and the products are heterogeneously distributed.

A common but erroneous assumption is that an age derived by one isotopic method should agree with an age derived from another mineral using another dating method; an ore deposit or vein should have 'an age' regardless of the dating method applied. However, different minerals and different isotopic methods measure different processes and events. Or, they may reach isotopic closure at different times during the same event. Three basic errors are common. First, in some cases, ages overlap within stated uncertainties, but are nominally different. Some authors overinterpret the nominal difference, overlooking the fact that the difference in age is not statistically significant. Second, different ages may be drawn from different minerals and/or different isotopic systems that experience isotopic closure under different conditions. Some authors use this as a basis to conclude 'clearly more dating is needed' or 'one of the ages must be wrong.' An example is a Re–Os molybdenite age from a sulfide–quartz vein and a $^{40}Ar/^{39}Ar$ age from sericitic alteration (e.g., Watanabe and Stein, 2000). Both ages are meaningful; the latter is younger because it records the final cooling for a hydrothermal–magmatic system in a thermally perturbed region. Third, some authors report ages without accompanying uncertainties, without analytical data, and even without stating method and mineral used for dating. In this case, there is no way to determine if ages actually differ, to assess quality of data and precision, and to evaluate validity of interpretation. Age data, like all data in science, must be published in a way that permits scrutiny.

Chronologies associated with a wide array of geologic processes can serve as records of metal mobility in the crust. We are able to date diagenetic and cementation processes that record the cycle of sequestration of metals from the hydrosphere into the geosphere (e.g., Georgiev et al., 2011), and episodes of fluid flow creating ore in sedimentary rocks (e.g., Rasmussen et al., 2007) can be dated. Geochronology documents burial and exhumation velocities for terranes important to ore genesis (e.g., Massonne et al., 2007). Dating of detrital zircon incorporated into sediments constrains the timing of subsequent
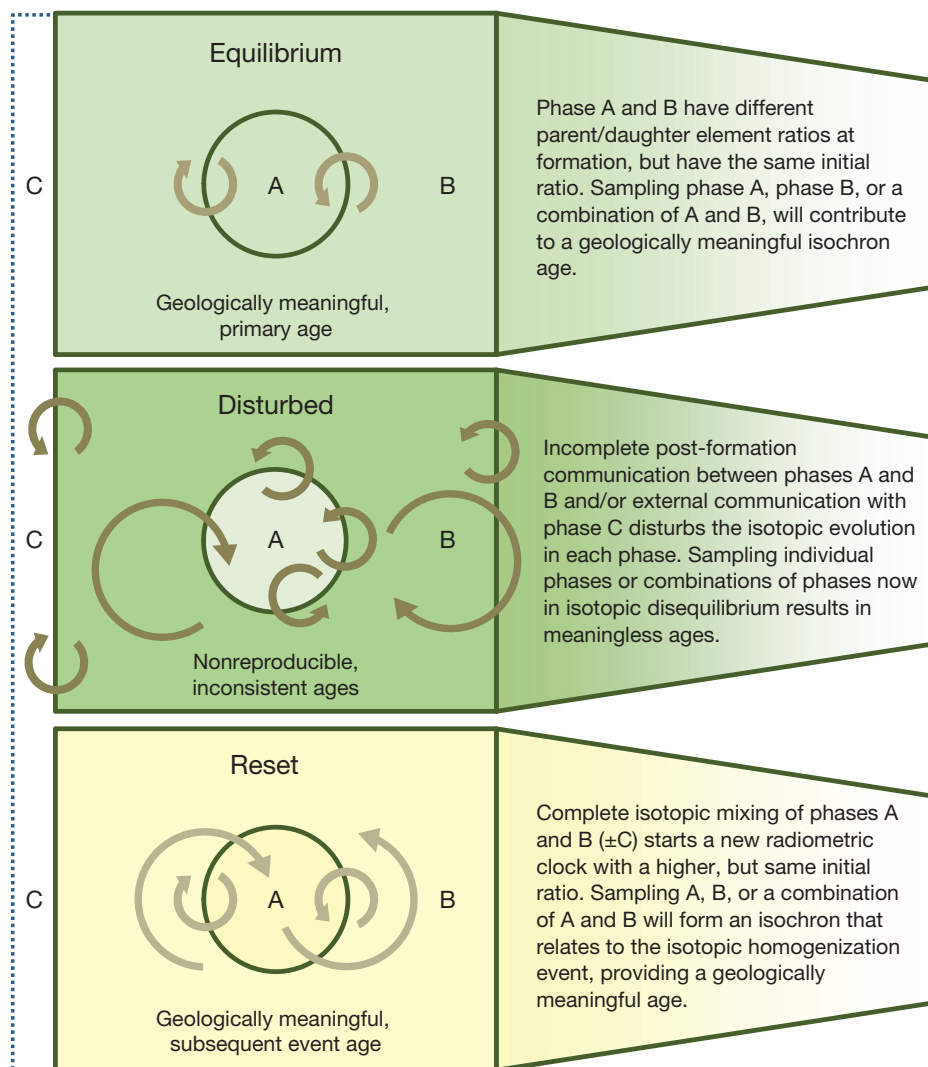
Figure 2 Concepts of equilibration, disturbed, and reset ages defined. The terms 'disturbed' versus 'reset' are commonly misused or incorrectly interchanged; these different terms represent different processes. Whereas reset ages give consistent results, disturbed ages do not on resampling the same material.

ore genesis (e.g., Cornell et al., 2009). Age archives retrieved from *pre*ore processes may expose metal-rich source rocks and enable an estimate of mineral fertility in geologic terranes (e.g., Bierlein et al., 2006a).

13.4.3.2 How Radiometric Clocks Work

The Re–Os isotopic system is used to illustrate basic principles of radioisotope geochronology, because of both its relative simplicity and its broad applicability to ore geology (Figure 3). For the Re–Os system, the accumulation of the daughter isotope may be stated mathematically:

$$^{187}Os_m = {}^{187}Os_i + {}^{187}Re_m(e^{\lambda t} - 1) \qquad [1]$$

where $(^{187}Os)_m$ = moles of the daughter isotope measured today, $(^{187}Os)_i$ = moles of the daughter isotope present at the time the clock started, $(^{187}Re)_m$ = moles of the parent isotope
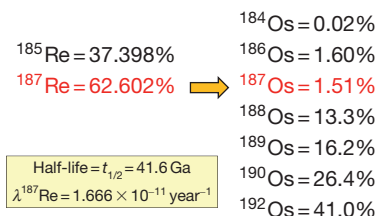
Figure 3 Isotopic composition of Re and Os in bulk Earth. Isotope ^{187}Re decays to ^{187}Os. The low abundance of ^{187}Os in bulk Earth makes accumulation of radiogenic daughter easy to measure.

measured today, λ = the decay constant, and t = time since the clock started. For single mineral clocks, a negligible amount of daughter element is incorporated into the mineral on formation: $(^{187}Os)_i \approx 0$. The number of variables in eqn [1] is reduced to one, and we can solve directly for time:
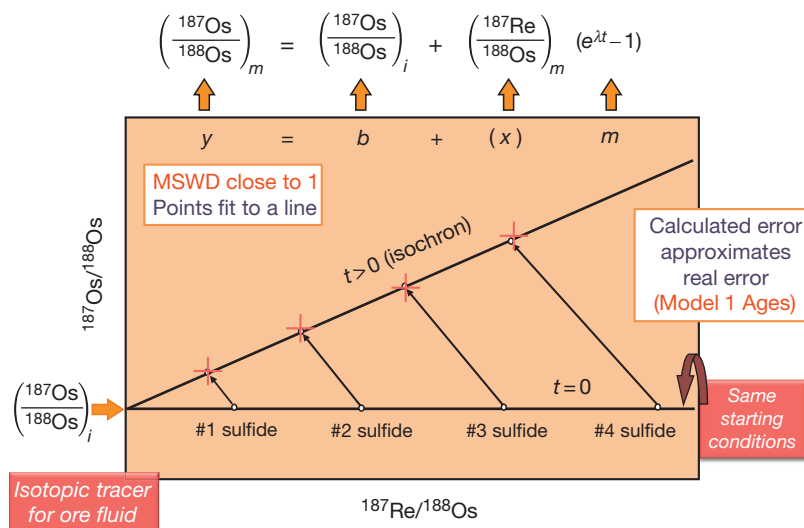
Figure 4 Mechanics of isochron diagram with explanatory isochron equation. Example shows linear regression of four data points (with similar analytical errors for illustration). Ideally, isochrons should be based on more than four points. See full discussion in text.

$$t = \frac{\left[\ln \left(\frac{^{187}Os_m}{^{187}Re_m} + 1 \right) \right]}{\lambda} \qquad [2]$$

In this simple example, note the critical underlying assumption – there is no gain, loss, or exchange of either parent or daughter isotope since the clock started.

Absolute concentrations of Re and Os isotopes are most commonly determined by the isotope dilution (ID) method. That is, a precisely weighed mass of sample is mixed with a precisely known amount of a 'spike,' a solution enriched in one or two isotopes of the same element. The most precise determinations of heavy isotope abundances are made by thermal ionization mass spectrometry (TIMS), which measures ratios of atomic masses at high precision. The most precise age calculations are made directly from the measured mass ratios, as converting to absolute concentrations for use in eqn [1] introduces uncertainties (e.g., weighing and spike calibration errors). To accomplish this, all terms in eqn [1] are normalized to a single stable isotope, for example, ^{188}Os for the Re–Os system:

$$\left(\frac{^{187}Os}{^{188}Os} \right)_m = \left(\frac{^{187}Os}{^{188}Os} \right)_i + \left(\frac{^{187}Re}{^{188}Os} \right)_m (e^{\lambda t} - 1) \qquad [3]$$

The ^{188}Os isotope is chosen because it is neither radioactive, nor is it the product of decay of any other isotope; that is, the abundance of ^{188}Os does not change with time. When Re–Os applications to geosciences were first developed, ^{186}Os was used for normalization. It was subsequently recognized, during a comprehensive study of Norilsk Cu–Ni ores, that ^{186}Os is produced by α-decay of ^{190}Pt (Walker et al., 1994, 1997), introducing a small error – especially in materials with relatively high Pt contents. The Re–Os community therefore agreed to normalize to ^{188}Os (summary in Shirey and Walker, 1998).

Not all minerals provide a single mineral clock. In fact, most minerals incorporate some daughter element on crystallization. It is not possible to directly determine how much daughter was initially incorporated into the mineral without applying the isochron approach (eqn [3]). To solve for two unknowns – time and $(^{187}Os/^{188}Os)_i$ – results from multiple cogenetic samples are plotted on an isochron diagram (Figure 4). Here the age equation defines a straight line on a simple X–Y plot of $(^{187}Re/^{188}Os)_m$ versus $(^{187}Os/^{188}Os)_m$. The slope of the line $(e^{\lambda t} - 1)$ is readily solved for time. The Y-intercept is referred to as the initial Os ratio, $(^{187}Os/^{188}Os)_i$. That is, the Y-intercept reflects a fictional sample with zero parent isotope, ^{187}Re, and hence no ingrowth of radiogenic ^{187}Os. The $(^{187}Os/^{188}Os)_i$ is the Os isotopic composition of the analyzed material at the time it formed. If, for example, we analyze minerals deposited together by an ore fluid in a simple vein, the initial $^{187}Os/^{188}Os$ reflects that of the ore-forming fluid – and this can be linked to the source and/or history of that ore fluid.

Three assumptions underlie use of the isochron method: (1) all samples formed at the same time, (2) all samples shared the same $(^{187}Os/^{188}Os)_i$, and (3) there has been no gain, loss, or partial exchange of either parent or daughter isotope since the clock started – that is, the system remained isotopically closed. Here isotopic closure is defined as the time at which diffusion of the daughter isotope out of the mineral has effectively ceased. Recall that the third assumption applies to single mineral clocks as well.

The following sections expand on these two basic approaches – the single mineral clock and the isochron approach – and outline the conditions that assure isotopic closure.

13.4.3.2.1 Ages through single mineral clocks

Powerful radiometric clocks are single minerals with extreme parent/daughter ratios housed in resilient time capsules that resist chemical–isotopic communication with their surroundings and that resist internal recrystallization. Very few minerals are reliably up to the task. In the ore-forming environment, two minerals that consistently qualify are molybdenite (Re–Os) and zircon (U–Pb). Molybdenites have extraordinarily

high Re/Os ratios ($>10^6$) on crystallization. Molybdenite is the only naturally occurring mineral that takes in significant Re while largely excluding Os. Thus, its 'initial Os' (also called 'common Os') is exceedingly low. Overgrowths and chemical-isotopic exchange are rare, but within-grain, parent-daughter decoupling may be an issue (see Sections 13.4.5.3.2 and 13.4.5.3.3). Zircon typically has high U/Pb ratios and is generally resistant to chemical exchange. But, there can be challenges with chemical zoning and recrystallized domains, or high concentrations of common Pb (see Section 13.4.4.1.1). Some K-rich minerals serve as single mineral chronometers based on decay of ^{40}K–^{40}Ar, but the ages reflect closure of the clock at a specific temperature rather than primary crystallization. That is, they are of great utility for elucidating thermal or uplift histories, but less accurate for primary crystallization ages.

Any single mineral age calculated with an assumed initial ratio is referred to as a 'model age.' Molybdenite model ages are extraordinarily robust, as the Os in molybdenite is almost always nearly 100% radiogenic daughter ^{187}Os; the assumed value for the initial $^{187}Os/^{188}Os$ ratio has no impact on the age calculation. It is possible to check routinely for common Os during analysis, as discussed below, although this cannot be done by labs using a 'common Os spike.' Identical model ages for multiple molybdenite samples from the same occurrence provide yet another test. If the samples are truly cogenetic and the ages are precise, regression of molybdenite data on a plot of parent versus daughter (e.g., ^{187}Re vs. ^{187}Os) will yield a straight line with slope proportional to age projecting through the origin – that is, with zero initial ^{187}Os.

13.4.3.2.2   Ages through isochrons

The isochron approach accommodates samples or minerals that incorporate both parent and daughter elements on crystallization. Critical to isochronous results is that all samples acquired the same initial isotopic composition at the same time. A best-fit line for data from multiple cogenetic samples, determined by linear regression, provides a test of this condition.

To generate plots and analyze statistics, many geochronologists rely on ISOPLOT, the freeware developed and regularly updated by Ludwig (2012). ISOPLOT employs the standard York fit (Model 1) if the analytical errors can account for the entire scatter observed in the data. If the scatter exceeds that attributable to analytical errors, the program defaults to Model 3, which assumes the additional scatter is introduced by variable $(^{187}Os/^{188}Os)_i$. If the variation in $(^{187}Os/^{188}Os)_i$ is relatively small, the age may still be sufficiently precise to address critical geologic questions.

Goodness of fit for the regression is indicated by the mean square weighted deviates (MSWD), which is a measure of data point displacement from the regression line beyond each point's analytical uncertainty. Analytical uncertainties are calculated by propagating uncertainties for weighing, spike calibrations, mass spectrometric measurements, and blank corrections. If the data show no significant scatter beyond their analytical uncertainties (i.e., no excess geologic scatter), then $MSWD \approx 1$ (Figure 4). If the $MSWD \gg 1$ (Figure 5(a)), there are two possible causes: (1) real geological scatter, or (2) calculated analytical errors are too small. If the $MSWD \ll 1$ (Figure 5(b)), then calculated analytical errors are almost

certainly too large. Commonly used terminology is 'over-estimation or underestimation' of analytical errors. This is misleading, as analytical error is a calculated and not a divined commodity. Further, assigning large blanket errors to data sets is incorrect and in doing so undeserved Model 1 ages may be generated for isochrons.

Isochron results should always be reported with uncertainties (at 2σ, or 95% confidence level) for both the age (slope of regression line) and the initial daughter ratio (Y-intercept), along with the MSWD. The geologic significance of reported uncertainties differs among ages calculated for different isotopic systems or by different methods using different data reduction schemes. The age uncertainty will depend not only on the analytical uncertainties and any inherent geologic scatter in the data, but also on the spread of data points along the X and Y axes – it is difficult to fit a straight line through a tight cluster of points. Further, the uncertainty on the initial ratio will be large if the isotopic ratios are large – it is difficult to target the Y-intercept precisely from a long way out (i.e., from data that lies far to the right on an isochron diagram). An isochron-generated initial daughter ratio less than that of primitive mantle, and negative initial ratios are clearly impossible; both imply some kind of disturbance (e.g., Yang et al., 2009). Importantly, the geologic significance of reported uncertainties differs among ages calculated for different isotopic systems, as they may employ different data reduction schemes.

True geologic variation in the initial ratio, whether $^{187}Os/^{188}Os$, $^{87}Sr/^{86}Sr$, or $^{143}Nd/^{144}Nd$, is a common source of uncertainty recorded by isochrons. On the other hand, this variation should stir us to thought. A fundamental assumption for the isochron method is that all materials plotted together have identical initial ratios. Many recent studies suggest that perfect isotopic consistency in the magmatic environment is the exception (e.g., Martin et al., 2010; Mathez and Kent, 2007; McLeod et al., 2012). What is imperfect in the magmatic environment will be transferred to associated ore deposits. Similarly, sedimentary rocks are fraught with variations in initial ratios, either because of varied detrital input or inhomogeneous hydrologic/diagenetic processes. Hence, sedimentary-derived and/or sedimentary-hosted ore deposits may also harbor small inherent variations in initial ratios.

13.4.3.2.3   Conditions for isotopic closure

Isotopic closure implies an end to exchange of isotopes between a material and its external environment. Two parameters control closure. First, declining temperature slows diffusion of elements out of the crystal lattice; eventually, diffusion rates are effectively zero and escape–exchange ceases. Second, isotopic exchange requires a pathway; if the mineral is not in contact with another phase (solid or fluid) that welcomes the element in question, then the element is not likely to leave its primary host. If the material to be dated undergoes recrystallization in response to P–T-compositional changes, then isotopes will be redistributed among newly crystallized phases, and even within the same phase.

Fluids facilitate element transport and bring new components into the picture. Diffusion and recrystallization are initiated and new mineral assemblages are formed. When elements exchange places isotopic clocks are at risk. Conditions for
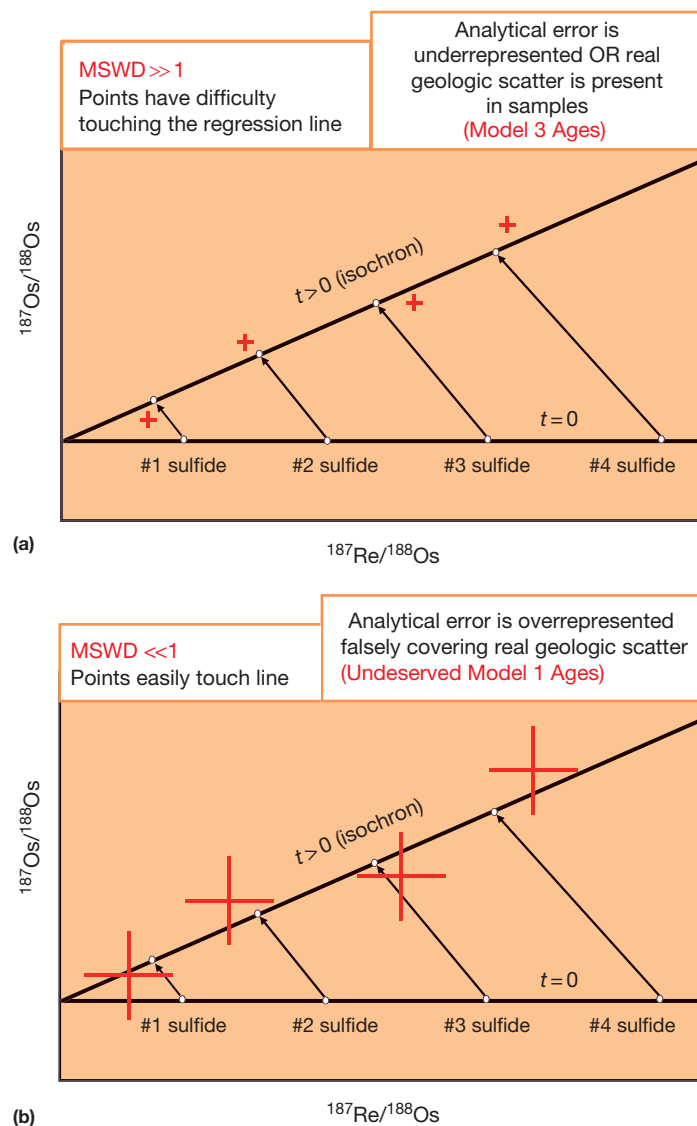
Figure 5 Isochrons with conceptual illustration of MSWD (mean square weighted deviates) and implications for Model 1 and Model 3 isochron ages as defined by Ludwig (2012). For any data point, uncertainty in X and Y are individually calculated values based on propagation of full analytical uncertainties (for illustration, crosses shown as same size). In reality, errors in X and Y are correlated (rho value) as ^{188}Os is a shared denominator in plotted X–Y values. Therefore, error crosses form ellipses (not shown here). (a) Underrepresenting the true analytical error for data points places undue penalty on the isochron uncertainty and MSWD value. (b) Overrepresenting analytical error, for example, in the erroneous practice of simply 'assigning' a generous error for all data points, produces regressions with apparent low MSWD and ages with undeservedly low uncertainties. In turn, this gives the false impression to casual users of isochron ages that the age must be accurate.

isotopic closure at the atomic scale are often overlooked by casual users of isotopic data. Too often lack of isochroneity is waved off as 'must be a mixing line' or 'disturbed age' or 'reset age.' These concepts should be understood in detail before being applied as an explanation for nonisochronous data. For example, mixing lines implies knowledge of endmembers, and reset ages and their associated initial ratios are usually geologically meaningful.

13.4.3.2.3.1 Thermal dependence

Closure of some – but not all – isotopic systems is temperature dependent. For example, the ^{40}Ar/^{39}Ar geochronometer is highly sensitive to thermal metamorphism. Argon is a noble

gas, not a structurally bound element in crystalline solids. Its residency in the solid–crystal lattice is tenuous. On heating, expansion of crystal lattices may allow escape of trapped radiogenic gas. Deformation exacerbates escape of gas. Temperature dependent chemical changes leading to recrystallization of mineral phases further compromise argon-based chronometry (e.g., Allaz et al., 2011). Nevertheless, under the right conditions, some minerals are highly adept at retaining radiogenic argon. Minerals most commonly dated by ^{40}Ar/^{39}Ar have associated closure temperatures below which argon is retained in the mineral on cooling. The closure temperature is also influenced by grain size and compositional variations within a mineral. The lower the closure temperature, the younger

the recorded age relative to the primary age. In general, hornblende retains argon at the highest temperature ($\sim 550\,°C$), followed by muscovite ($< 400\,°C$) and biotite ($< 350\,°C$), with K-feldspar able to leak argon to very low temperatures ($\sim 200\,°C$) (see review in Lee, 2009). To the extent that closure temperatures are well known, they offer a valuable tool for outlining the thermal history of a region. Minerals with low closure temperatures should not be assumed to reliably provide primary ages for ore-forming events.

The concept of 'closure temperature' has been applied to Re–Os dating of sulfides, implying a thermally dependent threshold for isotopic integrity. High closure temperatures have been estimated empirically for molybdenite (Bingen and Stein, 2003; Stein, 2006; Suzuki et al., 1996) and arsenopyrite and pyrrhotite (Demaiffe et al., 2013; Morelli et al., 2010), and experimentally for pyrite and pyrrhotite (Brenan et al., 2000). In the case of sulfides, however, chemical exchange rather than a thermal threshold is likely the trumping control on Re–Os isotopic closure.

As important as closure temperature is the 'container' for the mineral. Argon loss requires a pathway. In one example, quartz veins associated with Paleoproterozoic mineralization in the Cloncurry region yield demonstrably robust $^{40}Ar/^{39}Ar$ ages once corrections are made for any K-bearing minerals in the veins (Kendrick et al., 2006). Isotopic integrity is preserved, even with thermal and chemical overprinting – provided there has been no exchange (gain or loss of parent–daughter) beyond the volume of material taken for isotopic analyses. Similarly, sulfide minerals hosted in silicate rocks retain Re and Os regardless of chemical or thermal overprints simply because neither Re nor Os are soluble in silicates or *reducing* aqueous fluids; there is no driving force for these two chalcophile–siderophile elements to leave their sulfide host. For the Re–Os system in ore geology, the concept of thermal dependence and closure temperature is nearly irrelevant; what matters is chemical environment.

13.4.3.2.3.2   *Chemical dependence*

In most ore-forming environments fluids are prevalent and isotopic disturbance through chemical exchange may swamp other sources of error. Alteration is endemic to the ore-forming environment. Biotite is commonly chloritized and feldspars are commonly sericitized or saussuritized. Silica, sodium, and/or potassium may be introduced. The groundmass in altered ore-hosting rocks may little resemble its original composition. Isotopic disturbance may also depend on grain size; for example, fine-grained micas have a far larger surface area to volume ratio than coarse-grained equivalents, and are therefore more susceptible to exchange with fluids.

Nature's failure to reach and maintain equilibrium is a hallmark of dynamic geologic systems, and all but guarantees local variations in initial isotope ratios. Some geologic settings are conducive to prolonged fluid–rock interaction, which promotes isotopic exchange and may delay isotopic closure. In deep plutonic environments, deuteric alteration (igneous rocks maintaining late fluid phases) may introduce small variations in initial ratios, especially if high parent/daughter ratios characterize late magmatic fluids. That is, a small delay in isotopic closure may add radiogenic daughter to the initial ratio for minerals that crystallize late relative to earlier crystallized

phases. In addition, incomplete homogenization following magma mixing preserves isotopic heterogeneity. In sedimentary environments, chemical and isotopic exchange is expected during diagenesis. Variation in initial ratio is almost unavoidable. Decreasing porosity fills pore space with successive and/or replacing mineralogies. In the sedimentary ore-forming environment, intergranular deposition of sulfides and superimposed changes in the composition of sulfides may be part of the diagenetic process. In addition, introduction of external and sulfide-corrosive fluids can reopen porosity. In metamorphic settings, fluids released by dehydration or decarbonation reactions, typically with highly radiogenic isotope compositions, infiltrate and react with adjacent rock units. Sulfides in such settings can be very complex to date.

An example of challenges with chemical closure is Rb–Sr dating of sphalerite in sediment-hosted MVT (Mississippi Valley-type) Pb–Zn ores (e.g., Brannon et al., 1992; Nakai et al., 1990). Rb and Sr are abundant in sedimentary sections (especially Rb in shales and Sr in carbonates), and are readily mobile in saline fluids. The opportunity for chemical exchange between migrating ore fluids and sedimentary rocks in MVT settings is enormous. When the reservoir of parent–daughter elements in ore host rocks is large, the potential to introduce variations in the initial isotopic compositions of the ores becomes large. In the ore-forming environment, it is critically important to evaluate isotopic closure from the perspective of chemical closure. The changing stability of ore-associated gangue minerals, from alkali feldspars to micas to clays, quartz to calcite, and sulfides to oxides, provides a clear signal that the ore-forming environment is a playground of chemical growth and dissolution. Assumptions of widespread equilibrium underpinning some traditional ore deposit models are highly questionable.

Introduction of oxidizing fluids may reorganize sulfide compositions and ultimately remove sulfur and/or metals, including Re and Os. It is possible, however, to start a new clock without upsetting the original clock if the budget of Re and Os is largely retained in the originating system. As an analogy, evaporating a bit of water from the ocean has little impact on the water composition of the seas, but that bit of water vapor then develops its own history. As an example, at the Resolution Cu deposit in Arizona (Hehnke et al., 2012), secondary 20 Ma chalcocite (Cu_2S) with much lower Re concentrations may have partly derived its copper from the earlier 60 Ma porphyry Cu deposit dominated by chalcopyrite ($CuFeS_2$) and containing molybdenite (MoS_2) with typically high Re concentrations. In effect, some of the high grade chalcocite ore was 'self-sourced' in situ 40 m.y. later. The chalcocite took on its own clock essentially leaving nearly all of the Re–Os behind with primary chalcopyrite–molybdenite ores. The instigator proposed here may have been large-scale chemical modification of the earth's crust – that is, mild oxidation of the crust during widespread 20 Ma basaltic magmatism.

Sulfide encased in silicates or carbonates leaves no options for Re and Os except life in the sulfide structure. However, different sulfide minerals in contact with each another opens the possibility for Re–Os isotopic exchange. Another example, similar to the drop of water leaving the ocean and the Resolution Cu deposit described in the paragraph above, illustrates the effect of element migration when large concentration

differences are present. In Cu–Mo skarn deposits at Pitkäranta, Russia, molybdenites give reproducible ages of ~1800 Ma (Stein et al., 2003). Adjacent texturally related chalcopyrites in contact with the molybdenite give impossible ages up to 6 Ga! The relatively high-Re molybdenites have orders of magnitude more radiogenic daughter Os (^{187}Os) than very low-Re chalcopyrites of the same age. Molybdenite ages are not impacted by miniscule diffusive loss of radiogenic daughter, whereas the radiogenic Os budget in chalcopyrites is swamped by the tiniest uptake of ^{187}Os from the molybdenite. Thus, molybdenite ages remain robust, and chalcopyrite ages are erroneous and erratically older. In sum, the derivation of new or secondary sulfide minerals from preexisting sulfides or exchange of Re and Os among sulfides requires careful evaluation of the ore geology and paragenesis on a case-by-case basis.

13.4.4   Radiometric Clocks for Ore Geology

This treatise chapter focuses on methods that directly date sulfide minerals. The Re–Os chronometer is presented in Section 13.4.5, whereas the important U–Th–Pb chronometer, and the Pt–Os, Rb–Sr, ^{40}Ar/^{39}Ar, and Sm–Nd methods applied to ore geology are presented here. Emphasis is placed on advantages and disadvantages of each system relative to direct dating of the ore using Re–Os. Re–Os dating holds two advantages in most ore-forming environments: silicate minerals do not want these two elements and sulfide-stable crustal fluids do not mobilize them. On the other hand, recrystallization, metamorphism and mild oxidation imposed on earlier-formed sulfide assemblages may provide challenges. Each geologic situation merits independent evaluation before proceeding with dating. Each study should not lose sight of the complexities introduced by the absence of equilibrium in natural systems (e.g., Davidson et al., 2007; Jamtveit and Hammer, 2012).

13.4.4.1   U–Th–Pb (Uranium–Thorium–Lead)

No other technique has enjoyed as universal an application as U–Th–Pb. For example, detrital zircons bracket sedimentation ages, magmatic zircons and their cores and rims give us precursor, melt and crystallization history, rims give us postcrystallization history, and hydrothermal zircon gives us the record of fluid-rich events. In the ore-forming environment, simultaneous growth of minerals with high U/Pb ratios is one platform for dating ores, but often we are faced with teasing age information from complexly altered U–Pb minerals with a prior history. Even zircon may respond unpredictably and in surprising ways to overprinting events (e.g., Flowers et al., 2010). The U–Th–Pb chronometer in monazite is particularly susceptible to postdepositional fluids, but in this capacity can also provide valuable information on the time of fluid ingress if the monazite is fully reset (e.g., Williams et al., 2011).

Titanite (sphene) and rutile, CaTiSiO$_5$ and TiO$_2$, can form part of the magmatic, metamorphic, and hydrothermal record (e.g., Li et al., 2010; Rabbia et al., 2009; Romer et al., 1994). Since Ti is traditionally viewed as an immobile element, these two minerals have long been viewed as robust for U–Pb dating.

However, they are receiving increasing scrutiny in studies examining their solubility in metamorphic fluids; for example, rutile becomes soluble in high temperature Cl- and F-bearing brines (Rapp et al., 2010). Many of the experimental conditions used to track solubility and nucleation are not unlike the conditions in ore-forming environments. Still, use of U–Pb to date rutile (TiO$_2$) and cassiterite (SnO$_2$) deposits has been successful (e.g., Shi et al., 2012a; Yuan et al., 2011). The trio titanite–zircon–monazite has been dated to elucidate long-lived hydrothermal systems associated with talc mineralization (Poujol et al., 2010; Schärer et al., 1999). Collectively, some oxide, silicate, and phosphate (see Section 13.4.4.1.2) minerals, with due interpretive caution, give information on the age of ore deposition and/or earlier events potentially important to the ore-forming process.

13.4.4.1.1   Zircon (ZrSiO$_4$)

Because zircon is composed of silica and zirconium, two components abundantly present in most ore-related magmatic and metamorphic rocks, it has been used to bracket ore-forming events (e.g., von Quadt et al., 2011). That is, U-Pb ages for pre-ore and post-ore intrusions provide a duration period that encompasses, but exceeds, the mineralization history. It is also important to evaluate the zircon's postdepositional isotopic integrity. In general, zircon fares well, but ore-forming environments present a special case. An increasing number of studies highlight zircon vulnerability in regimes where fluids are present. For example, zircon may develop porous and convoluted granular textures, or recrystallized microdomains in the presence of alkaline-rich fluids (e.g., Kusiak et al., 2009; Rubatto et al., 2008). Subsolidus recrystallization of zircon at mid-crustal levels in association with muscovite compromises its isotopic integrety (e.g., Dempster et al., 2008). Recrystallized zircon rims have been attributed to fluid-rich chemical reaction fronts acquired 100 m.y. after zircon formation but in the absence of strong lattice strain and, remarkably, with preservation of original oscillatory zoning (Vonlanthen et al., 2012). Conditions that compromise zircon integrity are not unlike those in some ore-forming environments, and particular caution is needed for locations where multiple alteration and ore deposition events are spatially superimposed (see Section 13.4.5.5). In such cases, what steps can be taken to assure that the zircon analyzed staunchly represents the ore-forming event in question?

Unquestionably, reequilibration of zircon in the presence of aqueous fluids takes place (e.g., Geisler et al., 2007). Valley et al. (2009) distinguish younger ore-associated hydrothermal zircon from older magmatic zircon in the hosting granites. However, a common morphology or textural consistency between zircons in ore-forming environments has not been found (Schaltegger, 2007). In a comprehensive atlas of zircon textures, Corfu et al. (2003) emphasize the critical task of interpreting textures and properly assigning age domains to specific events; further, they raise the point that the category of 'hydrothermal zircon' is perhaps an artificial designation, since most metamorphic growth and resorption can be ascribed to fluid-rich encounters as well. Schaltegger (2007) amply states that there is no diagnostic morphology for hydrothermal zircon; that designation is best reserved for zircons

with clear coexisting hydrothermal assemblages (e.g., quartz vein host).

Zircons with high U/Pb ratios and correspondingly high radiogenic lead contents make for good radiometric clocks. However, zircon and other minerals used for U–Pb dating require assumption of an initial lead isotope ratio for single sample age calculations. This assumption becomes more critical for zircons with lower U/Pb ratios (see Section 13.4.5.6 for analog). It is seemingly logical to simply obtain the initial lead isotope ratio from presumed consanguineous lead-rich phases in the sample, but there are complexities with this approach (e.g., Romer, 2001; Romer and Xiao, 2005). If a Pb-rich phase growing in a hydrothermal or metamorphic environment acquires its lead from the breakdown of preexisting phases and/or from an evolving ore fluid, the initial Pb isotope ratio may not be constant throughout; further, it may not be representative of the initial ratio associated with zircon growth. Uranium-rich phases growing in the hydrothermal or metamorphic environments may face additional challenges derived from incongruent melting or mineral reactions, and inhomogeneous or incomplete retention or expulsion of intermediate elements critical to the U–Pb radiometric decay chain. Working with zircon in the ore-forming environment should provoke review of fundamental studies of zircon behavior; interpretation of 'hydrothermal zircon' is likely to be complex.

13.4.4.1.2   Monazite (Ce, LREE, Th, U, Ca)PO$_4$

Monazite is a common mineral in magmatic, metamorphic, and ore-forming environments. The isotopic integrity of this mineral, however, is easily jeopardized in the presence of fluid. Fluid-rich describes most ore-forming environments. Experimental studies using monazite of different grain size favor a dissolution–precipitation process over Pb volume diffusion (Teufel and Heinrich, 1997). Recent experimental work points to alkali-bearing fluids as the instigators of metasomatically induced textures in monazite, confirming a subordinate role of solid-state dissolution (Harlov et al., 2011).

Most ore-forming environments are characterized by Na and/or K alteration. The susceptibility of monazite to dissolution–reprecipitation in Na- and K-rich fluids should give pause to using this mineral, unchecked, for dating ore formation. If the monazite belongs to an earlier set radiometric clock, new crystallization – by any process – must be at a level where the initial Pb isotope ratio is reset at the scale of sampling. Incomplete isotopic homogenization internal to the grain on dissolution–precipitation and/or incomplete equilibration of new-forming monazite from externally introduced fluids will break the radiometric clock for both primary and secondary events.

In sum, know exactly what is being dated. Careful designation of monazite growth relative to tectonic fabric and decisive core–rim morphologies have been used to pin down the early metallogenic history for the giant Sukhoi Log Au deposit in Russia (Meffre et al., 2008). U–Pb ages for two morphologically different types of monazite and xenotime from the Guelb Moghrein IOCG deposit in Mauritania chronicle both late Archean and middle Proterozoic fluid events (Meyer et al., 2006). The details are important.

For monazite in particular, what is technologically possible in U–Th–Pb dating (e.g., Kohn and Vervoort, 2008) can unfortunately obscure important geologic uncertainty in some ore-forming environments. Kohn and Vervoort (2008) settled the overriding question of Eocene versus Miocene age for the Llallagua tin district in Bolivia. The reported 8.5% uncertainty in their age, however, shows how important geologic scatter is relative to analytical error. When applying geochronology to ore deposits, geologic scatter may be an important signal for understanding the ore-forming process; ages with large uncertainties should be independently evaluated for accuracy. Another example where analytical precision and geologic accuracy require careful evaluation is found in a growth–resorption dating study of monazite from the Challenger Au deposit in the Gawler craton, South Australia (McFarlane, 2006).

Although hydrothermal monazites have been used as a solo test for existing ore deposit models (e.g., Rasmussen et al., 2006), dating of several minerals from the ore-forming environment is a preferred approach. For example, paired molybdenite and monazite dating have been used to isolate fluid-rich events producing small mineral deposits in the Sveconorwegian of south Norway (Bingen et al., 2006), and a detailed dating study of zircon–monazite–xenotime from the Mole granite in NSW Australia suggests that a magmatic to hydrothermal transition spanned several million years (Schaltegger et al., 2005).

13.4.4.1.3   Uraninite (UO$_2$)

An obvious candidate for U–Pb dating is the ore-forming mineral uraninite. However, uraninite is not as amenable for dating as it might seem. Early studies of uranium deposits in collapse breccias in western United States produced imprecise ages, supported by scattered Pb–Pb compositions for galenas – all pointing to complex fluid pathways and metal sources (Ludwig and Simmons, 1992). Similarly, low-temperature uranium ores in tabular organic-hosted ore bodies and roll-front deposits record a long, complex history of U and Pb leakage combined with U adsorption and/or redistribution by interaction with oxidizing ground waters; as a result, the system is completely open to isotope exchange (Ludwig et al., 1984). Loss of fission gases are a phenomenon associated with disturbed uraninite U–Pb ages (e.g., Eikenberg and Köppel, 1995). Nevertheless, continued application of this method yields both geologically reasonable and isotopically disturbed and complex results (e.g., Alexandre et al., 2012; Förster et al., 2012; Romer et al., 2007).

13.4.4.2   Pb–Pb (Lead–Lead)

The ore mineral galena (PbS) contains essentially no uranium and thorium. Its lead isotopic composition is defined by ^{206}Pb (derived from ^{238}U), ^{207}Pb (derived from ^{235}U), ^{208}Pb (derived from ^{232}Th), and ^{204}Pb (stable). The U–Th history is simply inherited when galena forms and remains unchanged with passing time. Pb–Pb data for galenas are plotted in *X–Y* space as ^{206}Pb/^{204}Pb versus ^{207}Pb/^{204}Pb or ^{208}Pb/^{204}Pb, respectively (Figure 6). Thoriogenic lead (^{208}Pb) provides a parameter to look back at Th/U ratios in source rocks, whereas ^{206}Pb and ^{207}Pb provide a paired record of ingrowth from the decay of respective parents ^{238}U and ^{235}U. The premise is that extraction of lead to form galena must lead back to where parent isotopes ^{235}U and ^{238}U were in a unique ratio in the past. While Precambrian volcanogenic massive sulfide deposits are generally
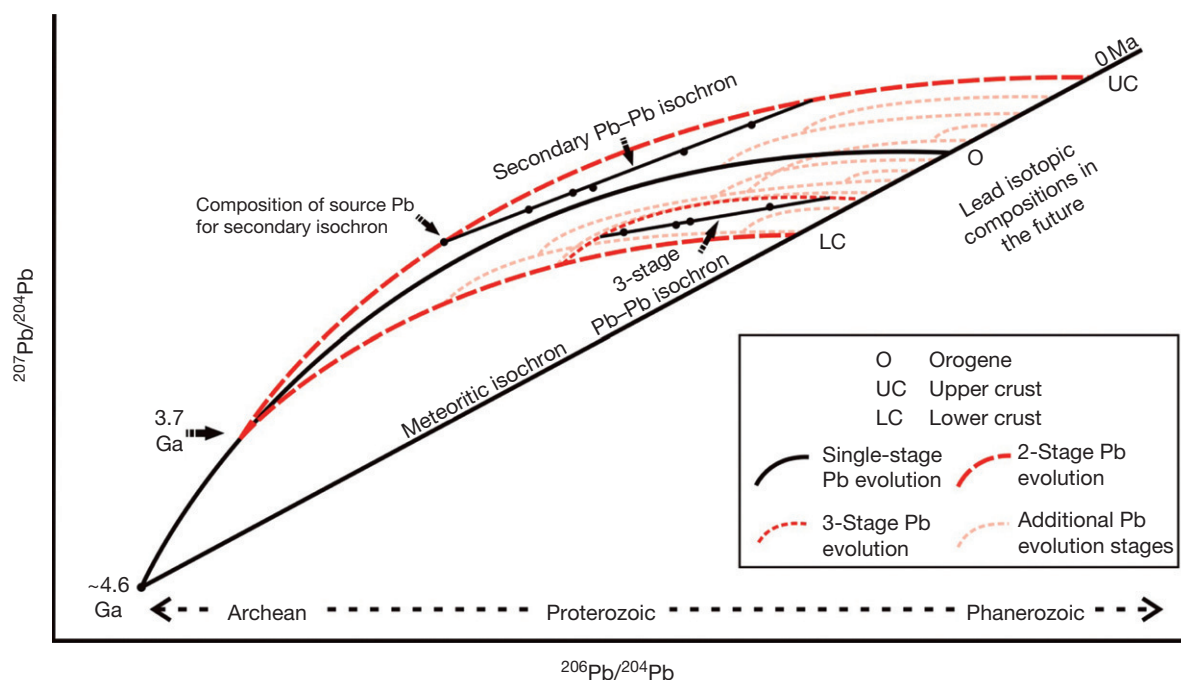
Figure 6   Schematic illustration of lead isotope evolution through time shows increasingly complex possibilities for U–Pb reservoirs in Earth's crust in younger rocks. In a traditional 2-stage model, Pb isotopes evolve along a simple curve from 4.6 to 3.7 Ga; at 3.7 Ga, crustal reservoirs are defined with higher (upper crust) and lower (lower crust) U/Pb ratios. In this model, Pb extracted at a later time as galenas from reservoirs with different U/Pb ratios will form a linear array (secondary or 2-stage Pb–Pb isochron); the lower intercept of the Pb–Pb isochron provides the age and composition of the source while the slope is related to the age of the galenas. If a third reservoir with a different U/Pb ratio is isolated at a later time, its Pb isotope evolution follows yet another set of curves; galenas forming from this reservoir yield a 3-stage Pb–Pb isochron. Further subdivision of U–Pb reservoirs further complicates interpretations. See text for discussion and stone-skipping analogy.

compliant, lead isotopic analyses of galenas from many other environments yield scatter on traditional Pb–Pb plots. Further, lead isotope data from galenas show increasing non-compliance with younger and younger samples, including Pb isotopic compositions for galenas from some Phanerozoic MVT ores that plot far into the future. Clearly, this is not realistic.

Increasing misfit of lead isotope data from galenas modified the concept of single stage bulk Earth Pb isotope evolution curves (Stacey and Kramers, 1975) and led to modeling a bulk Earth with increasing U/Pb ratio with time (Cumming and Richards, 1975). Still, the fit of galenas to this curve was not good for younger rocks. Subsequently, bulk Earth Pb evolution curves were replaced with individual lead evolution curves fitted to perceived histories for average upper and lower crust, and mantle, each with their own U/Pb ratio (Zartman and Haines, 1988). Source rock reservoirs with higher U/Pb ratios served to describe galenas with more radiogenic lead compositions, and reservoirs with long-term low U/Pb ratios described galenas with lower radiogenic isotopic compositions. An analogy for visualizing the history of lead extraction and preservation in galena (Figure 6) is presented:

A person good at skipping stones stands on the shore of a lake and casts his stone – first a big bounce, followed by another good size bounce, and another, with ten bounces before the stone drops to the lake bottom. Each bounce loses altitude and the last bounces are lower and closer together. The plunk to the bottom is extraction of the Pb into galena. The first high bounces represent much ^{207}Pb ingrowth early in

Earth's history with height representing a healthy presence of parent ^{235}U. With passing time, the proportion of ^{235}U, with its much shorter half-life, decreases relative to ^{238}U (present-day ^{238}U/^{235}U is 137.88; Faure and Mensing, 2005). Thus, after the first several bounces, the stone flies very low to the water and its horizontal vector dominates (curves flatten toward present day in Figure 6). More stone skippers arrive at the lake. Some of their stones give only three or four bounces whereas others give many more bounces; each stone travels on a different trajectory and different distances into the lake. If the lead isotopic compositions of the plunked stones (a.k.a., galenas) are measured, those farther into the lake will have more radiogenic lead isotopic compositions because their parental trajectories (a.k.a., U/Pb ratios) were longer – whether defined by height, number of skips, or both. It is possible that two stones will fly the same distance into the lake, but one may get there in four skips, and the other in eight skips. Obviously, they had very different flight histories, but their trajectories are lost once the stone sinks. Reconstruction of flight histories essentially vanishes once perturbed surface water on the lake quiets.

The high level of scatter in lead isotope data in ore-forming environments on Pb–Pb plots and the difficulty in assessing multireservoir histories back in time presents challenges for interpretation of lead isotope data (Figure 6). A stepwise Pb-leaching approach was applied to pyrrhotite associated with gold mineralization in Zimbabwe (Frei and Pettke, 1996; Frei et al., 2009), but this requires that the initial lead composition is homogeneous. Ages calculated from Pb–Pb isochrons are

generally imprecise, most likely because of the complexity of Pb isotopes and open-system behavior of both U and Pb in many systems (e.g., Jahn and Cuvellier, 1994). Therefore, use of Pb–Pb as a geochronological tool for ore geology has been replaced by more telling techniques in recent years.

Pb–Pb isochron diagrams may be very useful for evaluating effects of alteration and documenting direction of fluid flow and mixing. For example, the passive role of hosting country rocks at the site of ore deposition is clearly seen using lead isotope data from minerals within and external to giant porphyry Mo systems in the Colorado Mineral Belt (Stein and Hannah, 1985). As another example, the Pb isotopic composition of pyrites from the Siscoe gold deposit, Val d'Or district, Quebec, resembles the Pb isotopic composition of S-type granite host rocks (Olivo et al., 2007). Lead isotope data are perhaps more valuable for assessing geologic processes and relationships between ores and host rocks than for geochronology. Lead, as an element, is also used in trace element studies of ores, but the interpretive power of working with ratios of trace metals and lead isotope ratios is much greater than simple concentration data.

13.4.4.3 Pt–Os (Platinum–Osmium)

Ultramafic rocks, generally devoid of zircon and molybdenite, are notoriously hard to date unless rare baddeleyite (ZrO_2) can be found (e.g., Chamberlain et al., 2010). Parent isotopes for commonly used chronometers (U–Pb, Re–Os, Rb–Sr, and Sm–Nd) lack sufficient concentrations in the platinum group elements (PGE) environment. Walker et al. (1994) noted elevated ^{186}Os abundances in Pt-rich ores at Noril'sk, leading to full development of the ^{190}Pt–^{186}Os chronometer for geologic applications (Walker et al., 1997). Coggon et al. (2010) tested the ^{190}Pt–^{186}Os chronometer using the well-known Bushveld PGE-deposits, replicating the age within 2%. The relatively large age uncertainty reflects the $\sim$5% uncertainty in isotope ratio measurements made by laser ablation multicollector ICP-MS. Their attempt to date detrital PGE grains from Borneo yielded an uncertainty of >4%, possibly because the grains analyzed (museum samples) were of mixed origin. Nevertheless, the chronometer shows promise for constraining the age, and therefore the provenance, of both magmatic and placer PGE deposits.

13.4.4.4 Rb–Sr (Rubidium–Strontium)

The Rb–Sr chronometer applied to sphalerite (ZnS) was realized in the early 1990's (Brannon et al., 1992; Christensen et al., 1995a,b; Nakai et al., 1990). Shortly thereafter, Rb–Sr geochronology in the ore-forming environment began to fall out-of-favor as the residency and origin of Rb and Sr in sphalerite was challenged (e.g., Pettke and Diamond, 1996; Walshaw and Menuge, 1998). It became clear that for some deposits, sphalerite dating was impacted by the integrity of fluid inclusions which house much of the Rb–Sr budget, as neither Rb nor Sr are sulfide-forming elements. In a recent paper applying ^{40}Ar/^{39}Ar dating to fluid inclusions in sphalerite (Jiang et al., 2012), two distinct ages associated with crushing and gas release clearly demonstrate that sphalerite contains variably intact inclusions. Further, the likelihood for varying initial ^{87}Sr/^{86}Sr ratios during the course of sphalerite

deposition in the sedimentary environment was recognized. Other studies have used Rb–Sr to date pyrargyrite (Ag_3SbS_3), a silver ore mineral (Yu et al., 2009).

The Rb–Sr system has also been applied to hydrothermally altered sedimentary rocks containing quartz–sulfide veins with subsequent calcite–fluorite–quartz veins to produce a binary isotopic mixing model; this approach led to meaningful radiometric ages for processes characterized by isotopic disequilibrium (Schneider et al., 2003). Using Rb–Sr together with Re–Os dating at the giant Kipushi base metal deposit in the Democratic Republic of Congo, a convincing case for sphalerite chronometry is made (Schneider et al., 2007). Rb–Sr dating of base and precious metal-bearing quartz veins from the central Schwarzwald was used to construct a metasomatic history of element and ^{87}Sr/^{86}Sr isotopic exchange between hosting gneiss and veins (Glodny and Grauert, 2009); these data can be compared with U–Pb dating of Schwarzwald ore minerals (Pfaff et al., 2009) to examine the larger history of fluid activity in the region. Fluid infiltration and vein formation in the deep crust at granulite and amphibolite facies conditions have been eloquently addressed by Rb–Sr retained in chemically resilient 'containers' (Glodny et al., 2008), bringing this chronometer again to the forefront. This revival in Rb–Sr geochronology is leading to a deeper understanding of source rocks for ore geology.

13.4.4.5 ^{40}Ar/^{39}Ar (Argon–Argon)

For decades argon-based geochronology has been the main method for deriving age information in ore districts. The method is still in widespread use today as new and clever applications of ^{40}Ar/^{39}Ar geochronology for minerals with variable closure temperatures are used to examine cooling and uplift rates (Harrison and Zeitler, 2005). The ability of this chronometer to faithfully record and/or maintain primary ages in the ore-forming environment, however, has come under scrutiny. Some of the interpretive approaches, for example, use of 'preferred ages' and 'error-weighted averages of plateau ages' are questionable (Mauk et al., 2011). A plateau age, a user-selected interval in the argon release pattern based on specific statistical criteria (Ludwig, 2012), can be tagged with a precise analytical uncertainty. But precision is not proof of accuracy (see Section 13.4.1.3). Analytical uncertainty is a measure of the goodness of the laboratory and mass spectrometry part of the procedure. If a study advocates certain ages as 'preferred ages,' there should be a clear scientific explanation for the preference, and the event dated by the 'preferred age' must be defended by field or petrographic evidence.

The complexities of argon-based dating in the ore-forming environment are nowhere better seen than for the Pueblo Viejo Au–Ag deposit in the Dominican Republic (Arribas et al., 2011). The more ^{40}Ar/^{39}Ar dates acquired, the more elusive becomes the age of ore deposition using argon-based chronology. While ^{40}Ar/^{39}Ar is a marvelous tool for sorting out some geologic problems, it is not always the best approach for dating ore generation in magmatic–hydrothermal deposits, particularly if a long thermal history is involved. On the other hand, there are examples in the ore-forming environment where ^{40}Ar/^{39}Ar ages are in excellent agreement with accompanying Re–Os and/or U–Pb ages (e.g., Stein et al., 2005). In such circumstances, the agreement among two or three chronometers applied to the

same ore deposit can be used to argue for ore deposition that is directly tied to rapid cooling and/or uplift. Similarly, examples abound in which U–Pb ages target magmatic events, Re–Os provides the age of ore deposition, and $^{40}Ar/^{39}Ar$ completes the story with the postore thermal history. Multi-chronometer approaches hold great promise for sorting out the full geologic and thermal history surrounding complex ore systems.

13.4.4.6   Sm–Nd (Samarium–Neodymium)

The tungsten ore mineral scheelite ($CaWO_4$) has been used to date ore deposition in a variety of ore-forming environments. In almost every case, ages make geologic sense but are of low precision (e.g., Anglin et al., 1996; Bell et al., 1989; Darbyshire et al., 1996; Eichhorn et al., 1997; Frei et al., 1998; Kempe et al., 2001; Kent et al., 1995; Roberts et al., 2006). Limited spread in $^{147}Sm/^{144}Nd$ ratios is an underlying problem. Good isochrons require spread in plotted points; spread in points is achieved by variation in Sm/Nd ratios in the material being dated (see Section 13.4.3.2.2). Variation in Sm/Nd ratios generally corresponds to different chemical behavior of parent versus daughter elements. Because both Sm and Nd are REE and exhibit similar chemical behavior, the spread in $^{147}Sm/^{144}Nd$ ratios (X-axis on isochron) is limited. The typically low Sm/Nd ratios for scheelites may better constrain the initial $^{143}Nd/^{144}Nd$ ratio than the age.

$^{147}Sm–^{143}Nd$ dating has also been used to date fluorite deposits leading to sensible ages, but again with large uncertainties (e.g., Chesley et al., 1994; Turner et al., 2003). The same issue of limited spread in Sm/Nd in fluorites hampers precision. Comparative dating of fluorite and other minerals has made use of paleomagnetism (e.g., Symons, 1994); paleomagnetic dating is not addressed further in this chapter.

13.4.5   Rhenium–Osmium – A Clock for Sulfides

Rhenium–osmium (Re–Os) is the featured chronometer in this chapter because it provides the first widely applicable method for directly dating ore minerals (sulfides and oxides). Although the method was first applied to meteorites with their notable Re and Os concentrations (e.g., Shirey and Walker, 1998), its potential application to sulfides, and molybdenite in particular, has been known for more than fifty years. Re–Os sulfide dating by ICP-MS was revisted about 20 years ago, but results were compromised by analytical issues and poor precision. In the last ten years, Re–Os has become a powerful dating instrument, now widely accepted by the geochronology community.

13.4.5.1   Where We Find Re and Os

Re is a chalcophile and Os a siderophile element. Re is a sulfide-forming element, whereas Os is a PGE. Re and Os generally occur at the ppt level in the earth's crust with three notable exceptions – organic-rich shales, sulfides, and heavy hydrocarbons (Figure 1). A good place to find Os is the earth's core and extraterrestrial material. Earth's mantle contains ppb-to ppm-level Os primarily stored in sulfide and oxide minerals or in metal alloys such as osmiridium. The sulfide molybdenite is the only naturally occurring mineral in Earth's crust that consistently takes in Re at the ppm level.

Seawater provides a generally well-mixed reservoir of Re and Os that reflects the balance of inputs from continental erosion, seafloor magmatism and hydrothermal activity, and cosmic dust through Earth history (e.g., Peucker-Ehrenbrink and Ravizza, 2000). Organic material readily draws down Re and Os, giving these two elements short seawater residence times of 130–750 and 10–40 k.y., respectively (Colodner et al., 1993; Miller et al., 2011; Peucker-Ehrenbrink and Ravizza, 2000). Similarly, anoxic lacustrine environments also draw Re and Os into organic material and/or sulfides in bottom sediments. Therefore, organic-rich shales provide an Os isotopic record that can be tied to paleoenvironment. The effects of widespread mafic volcanism or meteorite impacts can be preserved in the ocean record (e.g., Schmitz et al., 2008; Turgeon and Creaser, 2008), and global increases in weathering of shale-rich sedimentary sections through Earth history may also be preserved in the marine record (Georgiev et al., 2012; Hannah et al., 2004a; Ravizza and Esser, 1993). These processes are fundamental to releasing, capturing, and sequestering metals. Plate tectonics brings these metal-laden sedimentary rocks into the deep crust and mantle where they mingle and mix with metals inherent to Earth's deep interior. These processes and the interplay of shallow and deep Earth environments are fundamental to understanding source rocks in ore geology.

13.4.5.2   Historical Background

The inherent promise of sulfide for highly accurate and precise Re–Os chronology was finally realized in the mid-1990s. Five major, analytically based issues were overcome: (1) difficulty equilibrating spike and sample Re and Os, (2) lack of sensitive mass spectrometry techniques, (3) lack of an interlaboratory age standard, (4) uncertainty in the ^{187}Re decay constant, and (5) poor stoichiometry of Os standard materials. Tackling these issues opened the door for Re–Os dating of sulfides in crustal rocks and took the field of economic geology in new directions.

13.4.5.2.1   Sample-spike equilibration

Laboratory methods moved from less reliable equilibration of spike and sample Re and Os by oxidizing alkaline fusion (Markey et al., 1998; Morgan and Walker, 1989) to high pressure and temperature sample dissolution and spike equilibration using inverse *aqua regia* in a sealed Carius tube (Shirey and Walker, 1995). Methods for more efficient Os recovery by distillation (Nägler and Frei, 1997) and solvent extraction using CCl_4 (Cohen and Waters, 1996) were developed for low level samples. High-precision chronology for low-Re and/or very young samples advanced rapidly with the development of a mixed-double Os spike ($^{185}Re–^{188}Os–^{190}Os$; Markey et al., 2003).

13.4.5.2.2   Negative TIMS

Many isotopic methods rely on measurements of positive ions in a TIMS. The switch to negative TIMS (NTIMS) (Creaser et al., 1991; Völkening et al., 1991) dramatically increased ionization of Re and Os, enabling very precise measurements of Re and Os isotopic compositions on picogram quantities. This advance was critical to opening Re–Os isotope geochemistry to crustal rocks.

It was many years before NTIMS became the standard, however. Most labs continued to use ICP-MS for Re–Os measurements. Re–Os age determinations by ICP-MS for a suite of molybdenites from southwestern North America (McCandless and Ruiz, 1993), for example, yielded unacceptably high external precision (reproducibility; ±6.8% at the 95% confidence level). Similarly, Re–Os dating of molybdenite by ICP-MS for several deposits in China (Du et al., 1995) yielded age reproducibility of ±3–4%. Microwave digestion and ICP-MS were applied to a suite of Japanese molybdenites (Suzuki et al., 1993, 1996) with reported errors of ±3–5%.

The ages achieved by ICP-MS dating made good geologic sense. Clearly, the Re–Os method was working on molybdenite, but a breakthrough in analytical technique was needed to achieve precision that could compete with that of ages determined by other isotopic methods. That breakthrough came with the switch to NTIMS, the standard for Re–Os dating of sulfides today.

13.4.5.2.3   An interlaboratory age standard

A major issue in bringing Re–Os chronology of sulfides to the geoscience community was the lack of a standard reference material for interlaboratory comparison. In-house molybdenite 'standards' developed in the 1990s by the AIRIE Program at Colorado State University were shared with other labs working to set up Re–Os dating for sulfides (e.g., Selby and Creaser, 2001). Simultaneously, Re–Os reference materials were being developed by chemist Du Andao and her colleagues in China. These reference materials were shared with and cocharacterized by the AIRIE Program (Du et al., 2004; Stein et al., 1997). Ultimately, a molybdenite reference material (RM 8599), a bulk sample from the mill at the Henderson Mo mine in Colorado, was fully characterized by AIRIE-CSU and University of Alberta, and brought to market through the United States National Institute of Standards and Technology (NIST; Markey et al., 2007). In sum, swapping of home-grown reference materials and achieving analytical agreement between three laboratories (Beijing, Colorado, Alberta), all working together, brought to reality the Re–Os dating of common sulfide minerals.

The molybdenite reference material (RM 8599) permits interlaboratory comparison of Re–Os age, not Re and Os concentrations, a challenge still faced in recent studies (e.g., Zheng et al., 2012). This concentration conundrum was known with construction of the first molybdenite isochron (Stein et al., 1997). A single *milled* powder of molybdenite from the Huanglongpu Mo–Pb deposit in China shows significant variation in Re and Os concentrations (∼4%) in 25 mg aliquots from a single well-homogenized 30 gm sample of molybdenite powder. The variation is most likely the result of spatial decoupling of parent Re and daughter Os within molybdenite crystals (Stein et al., 2003; see **Section 13.4.5.3.3**).

13.4.5.2.4   Half-life hurdles – the ^{187}Re decay constant

Establishing the half-life of a parent isotope with certainty is imperative for radiometric dating. Molybdenite, with its extraordinarily high Re concentrations, was shown to contain essentially pure ^{187}Os and negligible common Os, thereby providing the first reliable estimates of the half-life of ^{187}Re at about 43 ± 5 b.y. (Herr and Merz, 1955; Hirt et al., 1963). Using this half-life, the ages of 30 other molybdenites were

determined with precisions ranging from about ±2% in an Archean sample from Greenland to about ±15% in a 38 Ma molybdenite from the United States (Herr et al., 1967). Fifteen years later, the ^{187}Re half-life was determined at 45.6 ± 1.2 b.y. by assuming the slope of a meteorite isochron represented an age of 4.550 Ga (Luck and Allègre, 1982). Re–Os ages for 11 molybdenites based on this revised half-life showed that, in a few cases, ages were too old (some older than the age of the earth). These highly inaccurate results were attributed to Re loss due to metamorphic and/or hydrothermal processes (Luck and Allègre, 1982) – a major setback for Re–Os dating of molybdenite, as the chronometer was labeled as unreliable.

The half-life of ^{187}Re was again redetermined as 42.3 ± 1.3 Ga by measuring ingrowth of ^{187}Os over several years in a carefully purified kilogram of Re (as perrhenic acid, $HReO_4$; Lindner et al., 1989). Re-analysis of the same molybdenites that previously gave aberrant ages (Luck and Allègre, 1982) now produced ages in good agreement with wall rock ages determined by other isotopic methods, leading to the conclusion that earlier discordant results reflected sample-spike equilibration problems rather than issues with the molybdenite chronometer (Suzuki et al., 1992, 1993). It became clear that Re–Os dating of molybdenite held great promise.

Meanwhile, other groups were working to bring the Re–Os chronometer to fruition using ID-NTIMS (Stein et al., 1997, 2001a). Again, the half-life of ^{187}Re was called into question, as nearly all molybdenite ages acquired by the AIRIE Program and its earlier equivalent at the United States Geological Survey were consistently older (1.5%) than U–Pb ages for contemporaneous minerals. New estimates of the ^{187}Re half-life, accompanied by a much reduced uncertainty (Shen et al., 1996; Smoliar et al., 1996) led to today's widely accepted ^{187}Re decay constant of 1.666×10^{-11} year^{-1} with ±1.02% uncertainty (Smoliar et al., 1996); an uncertainty of ±0.31% may be used for the ^{187}Re decay constant if a lab's standard can be tied back to the University of Maryland standard used by Smoliar et al. (1996). This revised ^{187}Re decay constant, determined by the meteorite community, was unknowingly predicted and independently affirmed by those working toward successful NTIMS Re–Os dating of molybdenite. Molybdenite provided an independent test of accuracy for the Smoliar et al. (1996) ^{187}Re decay constant. Re–Os ages for molybdenite from magmatic–hydrothermal systems now fell perfectly in line with U–Pb ages from geologically confirmed, paragenetically contemporaneous minerals (e.g., Selby et al., 2007; Stein et al., 2001a). Re–Os molybdenite geochronometry was open for business.

13.4.5.2.5   Stoichiometry of Os standards

For those calibrating spikes against the same natural Re and Os standards used by workers in agreement on the revised ^{187}Re decay constant and its reduced uncertainty, any systematic errors due to nonstoichiometry in standards are effectively absorbed into the ^{187}Re decay constant. Thus, age results are directly traceable to meteorite ages determined precisely by other isotopic methods with well-known decay constants. By sharing laboratory standards and using the new NIST reference material for molybdenite (RM 8599), interlaboratory calibration can be achieved. The long-standing issue of the

stoichiometry of Os gravimetric standards, however, remains an issue (Markey et al., 2007).

13.4.5.3 The Last Steps for the First Chronometer for Ore Deposition

With analytical breakthroughs in place, several additional concerns remained to be tested to establish the credibility of a new chronometer. *First*, comparison of Re–Os ages with argon-based chronology in the ore-forming environment led to suggestions that Re–Os ages were simply inaccurate (too old; see Section 13.4.5.3.1). For example, in the Yilgarn Craton, a strongly advocated model asserted that all Au deposits formed in a narrow window of time at about 2630 Ma. This conclusion was based in part on argon chronology. Older Re–Os ages were labeled as 'impossible' until their confirmation by U–Pb ages forced relaxation of tightly held models. Two prominent examples are the 2760–2750 Ma Re–Os ages for the Leonora Au camp in the Eastern Goldfields terrane (Witt et al., 2002) and the 2714–2696 Ma Re–Os ages for the Boddington Au deposit in the Western Gneiss terrane (Stein et al., 2001b). *Second*, it seemed inconceivable to many workers that the intense alteration associated with the porphyry ore-forming environment could leave the Re–Os chronometer intact. But the chronometer survives, as demonstrated in Section 13.4.5.3.2. *Third*, Re–Os data for some molybdenites are less reproducible than others. This issue steered some workers toward strict protocols for sample size, rather than toward geologic considerations. The cause was traced to ^{187}Re–^{187}Os parent–daughter decoupling within molybdenite in certain geologic environments (see Section 13.4.5.3.3); it is the molybdenite occurrence and container, not the molybdenite sample size that matters. *Fourth*, use of the terminology 'model age' stirred the ore geology community; model ages can be extremely robust (see Section 13.4.5.3.4).

13.4.5.3.1 Comparison of Re–Os ages with other ages

Different chronometers endemic to different minerals in the ore-forming environment may record different processes. Each result must be evaluated on the basis of geology – the sole criterion for meaningful geochronology. For example, a study combining monazite and molybdenite chronology, undertaken in a detailed field context in south Norway, shows that both minerals carry records of fluid migration in the crust (Bingen et al., 2006). Monazite crystallization, however, can record many different kinds of magmatic, metamorphic, or hydrothermal events, so the field details and careful petrographic imaging are indispensable.

Prior to Re–Os dating, most ages in the ore-forming environment were acquired through argon-based dating (K–Ar and ^{40}Ar/^{39}Ar) of gangue minerals, related in space and presumably in time to sulfide ores. An early study questioned the credibility of the Re–Os chronometer because Re–Os molybdenite ages differed from presumably correct K–Ar ages for Proterozoic to Cretaceous stocks in hypogene to supergene ore environments (McCandless et al., 1993). In other studies the credibility of the Re–Os chronometer was selectively upheld and refuted based on comparisons with Rb–Sr whole rock and K–Ar mineral dating of ore-hosting rocks (Suzuki et al., 1996). It was soon noted, however, that argon-based chronology does not record the same events as Re–Os molybdenite chronology (Stein et al.,

2001a). In most cases the Re–Os ages are consistently and sometimes notably older than argon-based ages for gangue minerals (e.g., Selby et al., 2002; Stein et al., 2001a; Watanabe and Stein, 2000). In fact, molybdenite retains the sulfide crystallization age whereas argon-based chronology provides a useful record of the thermal history of the system.

13.4.5.3.2 Lack of effect of alteration on Re–Os systematics

Early on it was suggested that Re–Os systematics in molybdenite depends on 2H versus 3R polytype or may be disturbed by intergrowths of powellite [Ca(Mo,W)O$_4$] or secondary clay minerals (McCandless et al., 1993). Subsequently it was shown that polytype has no demonstrable effect on molybdenite Re–Os ages (Stein et al., 1998). Also, Re–Os analyses of pure hand-picked Mo-rich scheelite [Ca(W,Mo)O$_4$] from the Felbertal W deposit yield blank level Re and Os, particularly when Re-loving molybdenite is part of the W-bearing assemblage (Raith and Stein, 2006).

Another alteration effect is overgrowth of the type commonly observed in zircon. Although the reasons are unclear, multiple generations of molybdenite typically form discrete nuclei rather than overgrowths. The first recognition of molybdenite overgrowths was documented at the intensely deformed Malanjkhand Cu–Mo deposit in central India (Stein et al., 2004). Detailed petrography coupled to Re–Os dating showed rare overgrowths of undeformed molybdenite around a gnarled earlier generation of molybdenite (Stein et al., 2004). In a later study, molybdenite overgrowths were observed in an unusual pod of monazite–xenotime gneiss within a granulite facies paragneiss (Aleinikoff et al., 2012). Imaging techniques and detailed petrography are always recommended, particularly in cases where replicate Re–Os ages based on different mineral separates of a targeted molybdenite occurrence fall outside analytical error. Despite these unusual occurrences, detailed imaging and dating of molybdenite clearly shows that overgrowths in molybdenite are extremely rare.

Porphyry-associated molybdenite Re–Os ages are unwavering whether samples are derived from potassic, argillic, or phyllic alteration zones. Suzuki et al. (2000) suggested that the Re–Os chronometer is susceptible to chemical alteration by NaCl and NaHCO$_3$ solutions, based on single analyses (no replicates) of molybdenites exposed to each solution (Suzuki et al., 2000). This observation, if true, is important to tracing back to source rock and considerations of metal mobility.

13.4.5.3.3 Parent–daughter decoupling conundrum in molybdenite

Despite agreement between molybdenite ages and other geochronologic controls, occasional aberrant molybdenite Re–Os ages appeared for some samples. This conundrum baffled early efforts to develop the Re–Os chronometer for molybdenite. Empirical evidence suggested that aberrant ages must in some way be associated with spatial decoupling of daughter ^{187}Os from parent ^{187}Re *within single crystals* (Stein et al., 1998, 2001a). Specifically, coarse-grained molybdenite, fragments of molybdenite crystals, or thin cleavage sheets from large crystals gave the more erratic age results, whereas fine-grained molybdenite gave the more reproducible results. Total extraction of coarse-grained molybdenite crystals, however, and their homogenization into a single powder markedly improved age

reproducibility for course-grained samples. Thus, mounting empirical evidence led to microscale testing and ultimately the realization of spatial decoupling of [187]Re parent from [187]Os daughter.

Laser ablation ICP-MS analysis of large natural crystals documented highly variable ages for discrete spots (Košler et al., 2003; Selby and Creaser, 2004; Stein et al., 2001a, 2003). As predicted by those studies, Takahashi et al. (2007) determined that radiogenic [187]Os has a smaller ionic radius and hence higher diffusion rate than [187]Re, and is therefore likely to diffuse readily into structural defects in the crystal. Critically, the Os does not leave the crystal as it is highly insoluble in most enclosing minerals or reduced aqueous fluids (see also **Section 13.4.3.2.3.2**). In part, this is what makes the Re–Os chronometer so robust relative to other chronometers. That is, parent–daughter elements in other chronometers have mineralogic residency options.

Recognition of parent–daughter decoupling in molybdenite led to the 'whole crystal' analytical approach (Stein et al., 2003). That is, sampling of molybdenite should always incorporate whole crystals, rather than parts of individual grains. This does not imply a threshold minimum sample size of 40 mg, as suggested by Selby and Creaser (2004). Rather, the texture of the material and its geologic context dictate the sampling protocol (Stein, 2006). If the molybdenite separate is prepared by targeting a specific generation and removing crystals in their entirety, tiny sub-mm grains of molybdenite provide accurate and reproducible age results. These concepts, and loss in accuracy by taking unnecessarily large molybdenite separates in metamorphic settings, are further discussed in Stein (2006).

Spatial variations in Re concentrations within individual molybdenite crystals, likely generated during crystal growth, have long been known (Terada et al., 1971). Variation in Re concentration for replicate runs of the same molybdenite sample – even for finely milled, fully homogenized samples is typical (Markey et al., 2007). As a result the NIST Henderson Reference Material #8599 for molybdenite is for age, not Re and [187]Os concentrations. The seemingly universal variation in Re concentrations in molybdenite is testimony to chaotic volatile transport of Re in many ore-forming systems. Volatile transport also chaotically distributes Mo within vein systems, as documented by Mo isotopic studies of molybdenites (Hannah et al., 2007). The preference of Mo for vapor over liquid has been experimentally confirmed at conditions representative of the porphyry ore-forming environment (Rempel et al., 2009).

13.4.5.3.4 *Revival of model ages for geochronometry*

Though based on the same fundamental principles as other radioisotope chronometers, the Re–Os system has two unique aspects that give it special utility unlike any other dating system. Both Re and Os are essentially confined to sulfide, and crust-forming processes strongly fractionate Re into the crust. Thus, the majority of crustal environments have high to very high Re/Os ratios, and the correction for initial Os is generally small. This means that assumptions for initial Os ratios leading to calculation of model ages are forgiving. This feature is amply demonstrated in molybdenite, and is commonly characteristic of arsenopyrite and pyrite in some environments.

In the next section, by way of an annotated journey through a Re–Os data set for a suite of molybdenites, the concept of model ages, the assumptions for initial Os compositions, the achievement of accuracy, the role of precision, and an analysis of error are presented. All of these concepts are interrelated, and they are best illustrated through example.

13.4.5.4 Molybdenite Dating of a Young Porphyry Cu–(Mo) Deposit in Chile

Current Re–Os molybdenite chronology permits reconstruction of ore formation vein-by-vein to reveal the periodicity of ore-forming events in real time. So that analytical error does not cover real time differences between ore-forming episodes, geologically young deposits must be used to reconstruct ore-forming events within a deposit. Ideally, the analyzed molybdenites have exceptionally high Re/Os and contain no initial or common Os. Well-described molybdenites from a young, well-studied porphyry Cu–Mo deposit in Chile provide a perfect example.

The Los Pelambres Cu–(Mo) deposit in the high Andes of Chile is one of the largest in the world, with a 3- by 5-km Cu–Mo footprint and an alteration zone that can be traced more than 10 km from the deposit (Atkinson et al., 1996). Molybdenite-bearing vein samples acquired from the ore zone (**Figure 7**) were firmly categorized into traditional vein types based on long-held models ascribing time significance to EB→A→B→C→D veins in porphyry systems (e.g., Gustavson and Hunt, 1975; Sillitoe, 2010). Abbreviated descriptions of these vein types are summarized directly on **Figure 7(a)**. Few have questioned this widely accepted model of attributing time significance to alphabetized vein types (e.g., Harris and Golding, 2002). Briefly, the model for porphyry Cu deposits is based on brittle failure of host rocks leading to propagation of quartz–sulfide veins referred to as stockwork in ore geology. Larger breccia features are also commonly developed during host rock failure. Tracing mechanical stress over large non-homogeneous distances in the natural world presents a challenge, but detailed studies of crack propagation give insight (e.g., Livne et al., 2010). The time component offered by Re–Os dating of molybdenite along single veins and fractures (i.e. cracks) provides unparalleled insight into the construction of porphyry-style deposits.

Figure 7 weaves Re–Os molybdenite data and analytical information together with a direct look at the samples showing the excavation pit(s) where material for dating was extracted with a small hand-held drill. This paired information – sample descriptions and analytical details – should never be separated. The following sequence of paragraphs, each starting with commonly asked questions, provides the full 'how-and-why' overview of the most powerful chronometer in ore geology, that of Re–Os in molybdenite.

How much sample is needed? Grain size may present a first-order control on sample size, as whole crystals should be sampled to capture potentially decoupled parent and daughter isotopes (see **Section 13.4.5.3.3**). Second, sample size for a molybdenite separate is driven by Re concentration and age, as there must be enough time for ingrowth of daughter [187]Os if Re concentrations are low. In the case of Los Pelambres the age is known to be about 10 Ma (Atkinson et al., 1996). For any Re–Os analytical work, having some idea of age gives a first platform of starting information. Having some idea of the deposit type gives a second platform of

Annotated Re–Os results with photos for molybdenites from the Cu–(Mo) porphyry deposit at Los Pelambres, Chile

AIRIE run number	Sample name	Vein type[1] [field classification]	Age	Re (ppm)	[187]Os (ppb) [radiogenic Os]	OsC (ppb) [common Os]	Age (Ma)[2]	Age (Ma)[3]	Without λ, absolute error on age (Ma)[2,4]	With λ, absolute error on age (Ma)[2,5]
MDID-23	CH02-LP13	EB		303.4 (2)	36.64 (7)	0.5 (1)	11.531	11.516	0.025	0.044
MDID-24	CH02-LP13	EB		312.7 (3)	37.76 (6)	0.39 (9)	11.531	11.519	0.021	0.042
MDID-28	CH02-LP13	EB		296.0 (2)	35.72 (6)	0.35 (9)	11.524	11.513	0.022	0.042
MDID-27	CH02-LP10	EB		389.1 (3)	43.89 (5)	0.24 (7)	10.769	10.763	0.016	0.037
MDID-35	CH02-LP14	EB	*p*	513.4 (4)	57.9 (1)	0.4 (1)	10.771	10.764	0.021	0.039
MDID-26	CH02-LP18	A	*r* *e* *s*	362.3 (3)	40.34 (9)	0.6 (1)	10.633	10.617	0.026	0.042
MDID-36	CH02-LP20	A	*u*	258.0 (2)	28.75 (6)	0.33 (9)	10.641	10.628	0.024	0.041
MDID-31	CH02-LP1	B	*m* *e* *d*	268.4 (2)	29.67 (7)	0.4 (1)	10.556	10.539	0.027	0.042
MDID-32	CH02-LP2	B		262.9 (2)	29.06 (4)	0.21 (7)	10.557	10.549	0.017	0.037
MDID-33	CH02-LP3A	B	*y* *o*	727.5 (6)	83.41 (9)	0.5 (1)	10.949	10.943	0.015	0.037
MDID-34	CH02-LP3B	B	*u* *n* *g*	373.0 (3)	41.43 (7)	0.4 (1)	10.607	10.596	0.019	0.038
MDID-25	CH02-LP5	B	*e* *r*	450.7 (4)	51.2 (2)	1.4 (2)	10.852	10.822	0.050	0.060
MDID-41	CH02-LP4	D		221.2 (2)	23.51 (5)	0.27 (9)	10.147	10.135	0.025	0.040
MDID-29	CH02-LP6	D		236.5 (2)	27.27 (6)	0.38 (9)	11.009	10.993	0.027	0.044
MDID-40	CH02-LP17	D		105.76 (9)	11.28 (3)	0.05 (6)	10.186	10.182	0.028	0.042
MDID-59	CH02-LP15	D		364.2 (3)	45.31 (6)	0.41 (7)	11.880	11.869	0.019	0.042
MDID-70	CH02-LP15	D		455.8 (4)	56.79 (4)	0.56 (2)	11.898	11.886	0.012	0.039
MDID-84	CH02-LP15	D		389.6 (3)	48.46 (4)	0.50 (1)	11.877	11.864	0.013	0.039
MDID-39	CH02-LP16	D		763.4 (7)	95.35 (9)	0.28 (8)	11.926	11.923	0.016	0.040
MDID-60	CH02-LP16	D		703.8 (6)	88.0 (1)	0.8 (1)	11.937	11.926	0.021	0.043

[1] Vein classification made in the field by Sillitoe, Perelló, and Stein

[2] Assumed [187]Os/[188]Os initial ratio for age calculation = 0.2 ± 0.1

[3] Assumed [187]Os/[188]Os initial ratio for age calculation = 1.0 ± 0.1

[4] Analytical error only, fully propagated; does not include the more significant error associated with uncertainty in the [187]Re decay constant

[5] Full propagation of analytical errors combined with error derived from uncertainty in the [187]Re decay constant

Ages calculated using [187]Os = [187]Re $(e^{\lambda t}-1)$; decay constant (lambda) used for [187]Re is 1.666×10^{-11} year^{-1} (±0.31%, Smoliar et al., 1996)

Absolute uncertainties shown for concentrations and ages at 2-sigma level

Samples run using Carius tube dissolution with double Os spike to correct for common Os and mass fractionation

Sample weights for runs were 20–25 mg, except three were 16 mg (MDID-40, MDID-60, MDID-84), and one was 11 mg (MDID-70)

Dilution of molybdenite with quartz–silicate was minimized and most analyses represent pure or nearly pure molybdenite separate

Replicate analyses for LP13, LP15, and LP16 based on new mineral separates extracted from same vein affirm accuracy of the age result (see text)

Re blanks are 1.16 ± 0.03 to 8 ± 3 pg; Os blanks are 1.9 ± 0.1 to 3.2 ± 0.6 pg; [187]Os/[188]Os ratios for blanks are 0.24 ± 0.01 to 1.5 ± 0.9

Field-based vein classification in use for time–space relationships in porphyry systems — EARLY

EB veins = early biotite–quartz veins with molybdenite ± chalcopyrite; lacking alteration halo, irregular to planer margins

A veins = granular quartz veins with chalcopyrite ± bornite ± molybdenite; lacking alteration halos; non-planer mismatched margins

B veins = banded or symmetrical quartz veins with chalcopyrite ± pyrite ± molybdenite; matched planer margins; little alteration halo

D veins = vuggy open-space with pyrite ± chalcopyrite ± molybdenite and sericite ± pyrite halos; notable alteration halos — LATE

(a)

Figure 7 Illustrative tutorial on Re–Os chronology of molybdenite to combine with question–answer discussion forum in text. Annotated summary of Re–Os ages for fifteen molybdenite veins with five replicate analyses from the Los Pelambres Cu–(Mo) mine in Chile are linked to sample photos. (a) Re–Os data table features critical footnotes (discussion in text). All replicate ages based on new mineral separates from the same vein to assure accuracy, through reproducibility in age result.

information for spiking the sample correctly on the first try, as it is clear that different deposit types have characteristically different Re concentrations (Stein, 2006; Stein et al., 2001a). The amount of isotopic tracer (spike) added must be in a reasonable balance with the Re (and [187]Os) concentrations in the molybdenite so that the mass spectrometer can measure ratios precisely. Re concentrations in molybdenite from porphyry systems dominated by Cu are generally in the hundreds of ppm range (e.g., Stein et al., 2001a, 2004; this chapter), whereas concentrations in Cu–Au or Au–Cu systems reach into the thousands of ppm range (e.g., Braxton et al., 2012; Zimmerman et al., 2008). Ages being equal, it should be apparent that a molybdenite with 10 ppm Re requires far more sample for the analysis than a molybdenite with 1000 ppm Re. Stated another way, to precisely date a very young molybdenite, a high Re content assures plenty of radiogenic Os (e.g., Braxton et al., 2012). For dating older molybdenites, even sub-ppm Re concentrations are not problematic. In such cases 'time is on our side.' In sum, 1–100 mg of molybdenite is typically used for Re–Os dating. The geologic setting and age dictate the answer. There is no singular answer or a 'threshold value' for sample size.

CH02-LP10, DDH-1004, 481 m

EB vein, rosette mo + cp + bio in 3 mm qtz vein with no halo; half core broken along vein

CH02-LP13, 3065 N Bench

EB vein, 2 mm qtz vein with mo + bio + cp; cut by B vein in field

CH02-LP14, 3065 SW Bench

EB vein, 1 mm qtz + bio + mo veinlet with no halo

CH02-LP18, DDH1073, 51 m

A vein, Portezuelo breccia host with pegmatitic bio-chl + kspar + qtz + cp + bn + mag cut by qtz veins with cp + bn + mo

CH02-LP20, DDH-1078, 50 m

A vein, 7 cm qtz vein (inside arrows) with 1 cm mo blades + cp + bn + anh cutting pegmatitic-UST textures in Portezuelo breccia; host is chloritized bio + qtz + kspar + aplite

CH02-LP16, DDH-71, 112 m

D vein, red arrows point away from 2 mm qtz + mo + py vein with ser halo; D vein cuts py veins in sericitized host rock; lower view shows vein opened

CH02-LP1, Cachimba Norte sector, pit

B vein, coarse mo on margin of 1 cm qtz vein with traces py + cp; kspar halo; vein cuts biotite (EB) veinlets

CH02-LP2, 3065 N bench

B vein, 1 cm granular qtz vein with mo selvages and local mo center, trace py + cp

CH02-LP3A, CH02-LP3B, 3065 N Bench

B veins, cross-cutting, A is clear glassy qtz + diss mo + cp; B is granular qtz + massive mo + cp

CH02-LP5, 3065 SW Bench

B vein, vuggy qtz vein with mo + cp in intermineral porphyry; late-stage B vein as porphyry showed little veining

CH02-LP4, 3065 N Bench

D vein, vuggy qtz + ser + kspar + mo + cp tetrahedrons with local cc coating

CH02-LP15, DDH-71, 111 m

enlarged below

D vein, euhedral mo + ser + py in vuggy 3 mm qtz vein with ser halo cutting porphyritic host with intense sericite-pyrite alteration

CH02-LP17, DDH-22, 157 m

D vein, 6 mm qtz vein with py + mo and qtz + coarse musc halo; broken to expose mo

D vein, qtz vein with central patches of coarse py + cp + mo in vein center; sericite halo; vein broken to increase mo separate

CH02-LP6, DDH-1037, 231.5 m

(b)

Figure 7 (Continued) (b) Photos summarize key aspects of dated samples. Dashed yellow circles show drill pits where molybdenite was excavated for Re–Os analysis (for some photos pit is outside field of view). Traditional classification of vein types and sample descriptions were firmly assigned on site in the mine pit and during sampling of drill core in February 2002 by R. Sillitoe, J. Perelló, and H. Stein. Vein types follow the traditional field nomenclature of Gustavson and Hunt (1975) as summarized in Sillitoe (2010). Objective was to compare Re–Os radiometric ages with field-based assignment of relative time.

Finally, as an important side note, Re concentrations reported for molybdenite in the literature may not necessarily reflect the true Re concentration for pure molybdenite; a molybdenite separate may be diluted 95% or more by silicate minerals without compromising age integrity. In the last decade, the objective of most Re–Os work on molybdenite has been solely for the purpose of age. Thus, the silicate dilution in molybdenite separates was not consistently reported.

Why is no isochron presented for the Los Pelambres Re–Os data? The Los Pelambres Re–Os data show high-precision, statistically distinct model ages for carefully selected individual occurrences of molybdenite extracted from well-documented vein sets, mutually determined by experts in the field (**Figure 7 (a)**). To plot these data together on an isochron is to discard detailed age information on the construction of porphyry systems, and instead present a rather meaningless and less precise average age.

What about dating coprecipitating chalcopyrite or pyrite to confirm the Re–Os molybdenite ages? Some early studies presented data for nonmolybdenite sulfides in porphyry environments claiming information can be gained about the initial Os ratio. This approach has little to offer. If molybdenite is a coprecipitating sulfide then other sulfides cannot compete for Re. In a young deposit, taking on a mineral with low Re means poorly determined radiogenic Os. If common Os is present, determination of the radiogenic fraction of Os is even more difficult. Attempts should not be made to construct isochrons from data that are dominated by Re and Os blank (e.g., Barra et al., 2003), particularly when molybdenite is available. In addition to an inevitable loss of precision, loss of accuracy and a meaningless $^{187}Os/^{188}Os$ intercept (initial Os ratio) may result. Once published, data are susceptible to misuse if the limitations of the method and blank/sample ratios are not clearly known and understood by the users.

As an important side note, blanks should never be simply assumed and applied as a blanket correction to a Re–Os data set. Blanks are derived through isotopic measurement and are uniquely applied to data for individual samples. Because Re and ^{187}Os levels are so high in molybdenites, blank normally has no effect on determined concentrations (and therefore ages). For sulfides with low Re and Os concentrations, however, proper blank assessment and correction are essential.

What does the common Os show and when is this important? In the Los Pelambres example, common Os is calculated through use of a double ^{188}Os–^{190}Os spike. The radiogenic ^{187}Os is measured against ^{188}Os in the spike, while common ^{192}Os is

measured against [190]Os in the spike (Markey et al., 2003). Most molybdenites have essentially zero common Os, or an amount that falls inside the analytical error for measured radiogenic [187]Os. For the Los Pelambres molybdenites, a small amount of common Os is present at levels up to about $10\times$ the analytical error for the [187]Os (Figure 7(a)). But the component of [187]Os in the common Os is very small, as [187]Os is about 1.5% of bulk Earth Os. Nevertheless, the double spike allows us to subtract the common [187]Os from the total [187]Os, providing us with only the radiogenic [187]Os derived from decay of [187]Re. An accurate number for the radiogenic [187]Os is used for the age calculation. This is the most correct approach and for some molybdenites, with truly significant common Os ($>$10%!), this approach is essential.

What does it mean when reference is made to a Re–Os age with the decay constant uncertainty included or not included? The decay constant uncertainty can be omitted from reported errors on ages when comparisons are made between samples that have been dated by the same isotopic method. For Re–Os, the dominance of the uncertainty in the [187]Re decay constant relative to measured analytical error is clearly seen (compare columns in Figure 7(a)). Including the decay constant uncertainty when comparing Re–Os to Re–Os model ages, in effect, inflates the error on the age for every sample. Note that the calculated absolute age is the same in either case. Comparison of Re–Os ages between Los Pelambres molybdenite samples justifies use of just analytical error to delineate individual molybdenite depositional events. However, comparison of Re–Os ages with U–Pb ages, for example, requires reporting the larger, combined analytical plus decay constant uncertainties. To assure that data are not misused or misrepresented, reporting the full error (combined analytical plus decay constant) should be the default.

Prior to widespread application of the Re–Os molybdenite chronometer, U–Pb ages were the standard. Because U–Pb ages were compared with other U–Pb ages, propagation of the decay constant uncertainties for parent isotopes [238]U and [235]U into reported errors on U–Pb ages was often omitted. But comparison of ages between different isotopic systems (e.g., U–Pb and Re–Os) requires that full uncertainties are included in the stated errors for ages (Bergemann et al., 2001). In addition, the statistical treatment of analytical data differs with isotopic system and approach. For example, a large number of dated spots ablated from a population of zircon crystals can provide a very small analytical uncertainty compared to the isochron approach. This important topic is not covered further in this chapter.

How do we assess accuracy in a Re–Os result? Deposition of discrete molybdenite crystals along cm-scale distances in veins in the porphyry environment provides an excellent test for accuracy. At Los Pelambres, this approach was essential when surprisingly old ages were obtained for D veins that are universally classified in the field as the youngest veins in the Cu porphyry ore-forming environment. Replicate dating of unique mineral separates acquired from the same vein were made for three Los Pelambres molybdenite vein samples (LP13, LP15, LP16; yellow and green highlighted boxes in Figure 7(a)). The age agreement is extraordinary and well inside calculated analytical errors. *Replicate dating from the same mineral separate tests analytical precision only. Replicate dating for spatially distinct mineral separates derived along a natural vein tests accuracy of the age.*

If the isotopic system was not closed, it would be impossible to exactly reproduce ages for different molybdenite separates along a vein.

As an additional test for accuracy, two visibly cross-cutting molybdenite veins from a single hand specimen (blue boxes, Figure 7(a)) were dated. Both were classified as B veins in the field. In agreement with cross-cutting relationships (Figure 7(b)), the earlier molybdenite-poor quartz vein is $\sim$350 000 years older than the later molybdenite-rich quartz vein. Re–Os dating pins absolute ages on relative time relationships; in doing so geologic accuracy is tested and confirmed.

If common Os is present, how do we know its initial Os isotopic composition? For essentially all molybdenites the assumption of a common Os isotopic composition has negligible effect on the age calculation. At Los Pelambres, where a measurable bit of common Os is present, the effect on the age for two different assumed common Os compositions can be assessed (Figure 7(a)). A small systematic difference in calculated ages is shown by comparing a common Os isotopic composition of 0.2 (e.g., mantle-dominated source) to a ratio of 1.0 (e.g., eroding continental crust today). A 'systematic difference' means that nominal ages are all shifted in the same direction. More importantly, the systematic differences are well inside calculated analytical errors. The persistent presence of common Os in Los Pelambres molybdenites is an interesting observation, and highlights the merits of using the double Os spike for dating molybdenites. In some studies a whiff of common Os can be attributed to a trace of chalcopyrite or pyrite in a molybdenite separate, but the consistent presence of common Os in all Los Pelambres analyses clearly shows that this explanation cannot be employed.

13.4.5.4.1   Full circle back to the field

The Re–Os data suggest that sulfide deposition at Los Pelambres was episodic over a period of at least 1.85 m.y. and almost certainly considerably longer. It is unreasonable to think that this study captured the first and last vein events at Los Pelambres. While a time span of about two million years is useful information, it does not dictate the duration of ore-forming systems for similar deposits at other localities.

Knowledge of absolute time together with detailed geologic descriptions and context for the dated samples (Figure 7) may be used to test field-based models for the genesis of porphyry-style Cu deposits. In the Los Pelambres example, assigning relative time in the field on the basis of vein type or vein alteration halos leads us astray. For example, the oldest Re–Os ages at Los Pelambres (CH02-LP15 and CH02-LP16; Figure 7(a)) are from veins firmly classified as D veins, which, according to the model, should be youngest. Further, these oldest D veins cut strongly sericitized host rock, suggesting that even earlier alteration–mineralization events are present (e.g., CH02-LP16; Figure 7(a)). Therefore, significant Cu mineralization is associated with events that preceded classically described main ore-stage A and B quartz–sulfide veins. The presence of an early sericitization event (prepotassic alteration) indicated by 'green mica veins' and 'Type 4 veins' in fact was recognized in a detailed paragenetic study by Atkinson et al. (1996); they also clearly recognized the importance of this early sericitization to the widespread onset of economic Cu mineralization.

In sum, porphyry deposits are not derived from an orchestrated sequence of time progressive vein types (EB→A→B→C→D) and unidirectional alteration sequences. Unless there is a cross-cutting relationship in hand specimen or at the outcrop, time cannot be extrapolated through intervening space. The Re–Os ages for molybdenite-bearing veins at Los Pelambres yield surprising results and show a previously unrecognized spatial–temporal complexity to ore deposition that is independent of perceived vein sequences and alteration halos. Of course, every vein cannot realistically be dated, nor can every ore-forming event within a large porphyry system. But it is clear that while so-called D veins are forming in one location, so-called A veins are forming in another, and the localities need not be far apart. This gives a new basis for evaluating ore-forming models in porphyry environments.
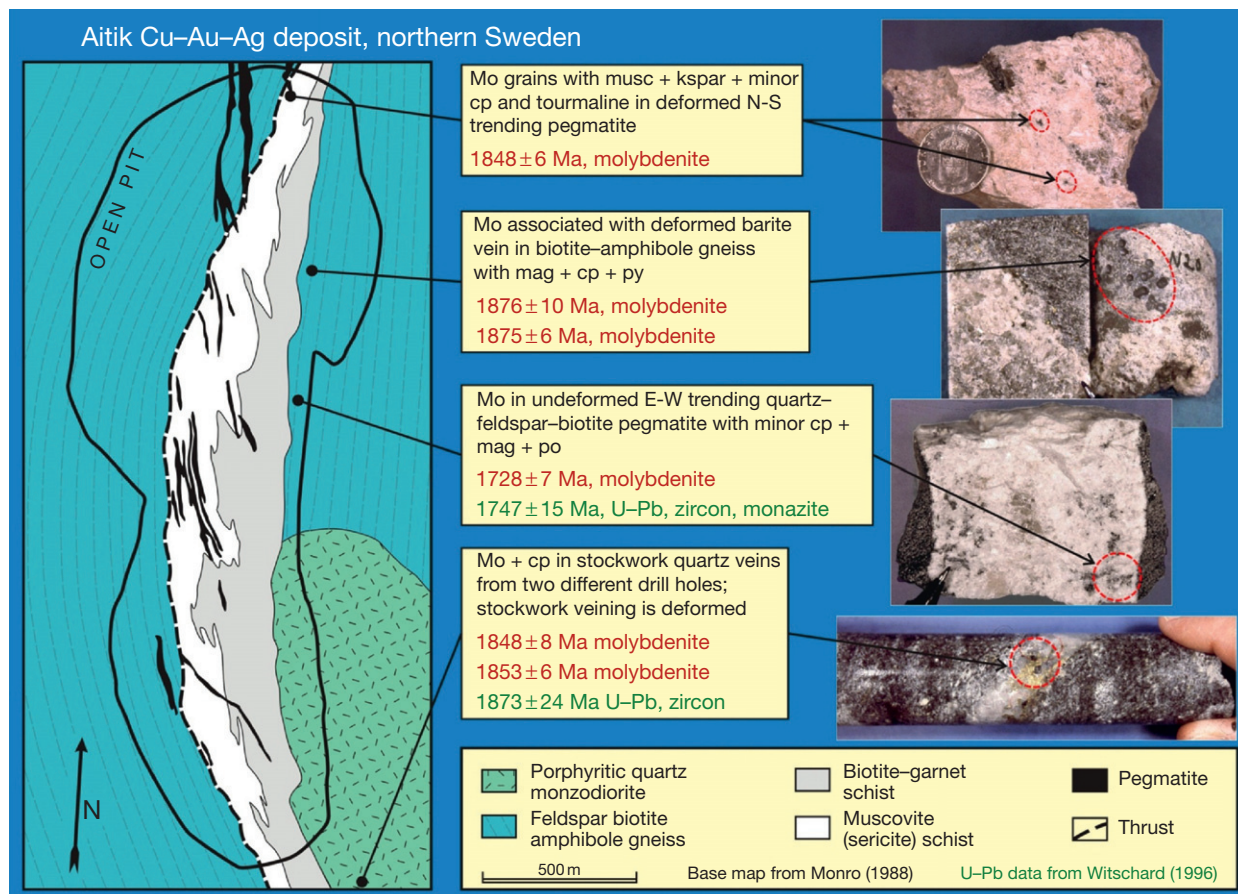
13.4.5.5 Molybdenite Dating of an Old Porphyry Cu–(Mo) Deposit in Northern Sweden

The time resolution possible for Re–Os dating of molybdenite from a geologically young system has been demonstrated with the Los Pelambres example. The oldest dated molybdenite (Spinifex Ridge, East Pilbara; Stein et al., 2007) is

Paleoarchean, and does not permit time resolution of stockwork vein events because the best achievable uncertainty on a 3.3 Ga age is about ±11 m.y. At the terrane scale, Re–Os dating of magmatic–metamorphic molybdenite can be used to reconstruct dehydration melting and fluid-rich events covering timescales of tens to hundreds of millions of years (e.g., Bingen and Stein, 2003; Stein, 2006; Stein and Bingen, 2002).

At the Paleoproterozoic Aitik Cu–Au–Ag deposit (Wanhainen et al., 2005), molybdenite is used to date multiple events within the 2.0–1.7 Ga Svecofennian orogeny; all dated molybdenites were taken in a clear geologic context from within this single highly deformed deposit (Figure 8). Analytical errors of ±4–8 m.y. and one at ±10 m.y. (rerun with corrected spiking reduced error to ±6 m.y.) include the ^{187}Re decay constant uncertainty (Figure 8). It is clear that these data do not permit vein-by-vein time resolution as was attained for Los Pelambres, but they do bring to light another important aspect of the Re–Os chronometer in molybdenite for ore geology: detailing the combined magmatic–metamorphic history to assess the larger metallogenic picture.

As shown in Figure 8, the resolution in Re–Os dating far exceeds that of U–Pb dating (Witschard, 1996) in this complex terrane, but the two dating methods roughly reinforce one

Aitik Cu–Au–Ag deposit, northern Sweden

OPEN PIT

Mo grains with musc + kspar + minor cp and tourmaline in deformed N-S trending pegmatite
1848±6 Ma, molybdenite

Mo associated with deformed barite vein in biotite–amphibole gneiss with mag + cp + py
1876±10 Ma, molybdenite
1875±6 Ma, molybdenite

Mo in undeformed E-W trending quartz–feldspar–biotite pegmatite with minor cp + mag + po
1728±7 Ma, molybdenite
1747±15 Ma, U–Pb, zircon, monazite

Mo + cp in stockwork quartz veins from two different drill holes; stockwork veining is deformed
1848±8 Ma molybdenite
1853±6 Ma molybdenite
1873±24 Ma U–Pb, zircon

Porphyritic quartz monzodiorite
Feldspar biotite amphibole gneiss
Biotite–garnet schist
Muscovite (sericite) schist
Pegmatite
Thrust

500 m   Base map from Monro (1988)   U–Pb data from Witschard (1996)

N

Figure 8 Use of molybdenite Re–Os chronology to resolve a larger metallogenic picture for the Aitik Cu–Au–Ag deposit, northern Sweden. A porphyry-style origin can explain the geometric relationship of exposed intrusions relative to biotite–garnet and muscovite–sericite schists (proposed potassic and phyllic alteration, respectively; Monro, 1988). Re concentration data for molybdenites suggest the superposition of two porphyry systems. See text for discussion.

another. That is, Re–Os molybdenite ages track fluid release events, whereas U–Pb ages indicate magmatic or metamorphic crystallization ages. Based on mapping and geologic interpretations proposed in Monro (1988), a three-phase history can explain the combined Re–Os and U–Pb data: (1) A 1.9 Ma quartz monzonitic precursor (Wanhainen et al., 2006) was the site for porphyry Cu–Au mineralization at 1875 Ma; this deposit was subsequently intensely deformed. The porphyry origin is supported by very high Re concentrations in 1875 Ma molybdenite ($\gg$ 2000 ppm, when corrected for dilution) and the association of this molybdenite with magnetite–chalcopyrite–pyrite–barite; (2) A second porphyry Cu–Au–Ag deposit with classic capping alteration, preserved as biotite–garnet schist (potassic) and muscovite–sericite schist (phyllic), is associated with a younger quartz monzodiorite intrusion at 1850 Ma; this interpretation is based on Re–Os dating of two modestly deformed stockwork quartz–chalcopyrite–molybdenite veins, and Re–Os dating of a deformed pegmatite (potassic alteration zone). Corrected for dilution, Re concentrations in vein molybdenites are >1000 ppm and >500 ppm for pegmatite molybdenite. Deformation of 1850 Ma magmatic–hydrothermal features followed, but the timing of this and earlier deformation events is not captured in the samples dated here; (3) A much later postdeformation event at about 1730 Ma produced undeformed, cross-cutting molybdenite-bearing pegmatite veins at Aitik.

If the interpretation of two-stages of porphyry Cu–Au mineralization at 1875 and 1850 Ma is correct, then Aitik is significantly younger than the well-known $\sim$1890 Ma Skellefte porphyry Cu–Au deposits associated with a volcanic arc to the south; in turn, this suggests unrecognized arc magmatism that may have been active for 15–40 m.y. Comparable timescales for less deformed analogs can be found today, for example, in the Andes. If this interpretation is not correct, then the Re concentrations associated with these 1875 and 1850 Ma molybdenites at Aitik need explanation, as nonporphyry and metamorphically derived molybdenites of similar ages in northern Sweden and globally have much lower Re concentrations, even into the sub-ppm range (Stein, 2006).

13.4.5.6 Low Level, Highly Radiogenic (LLHR) Sulfides

Low level, highly radiogenic (LLHR) sulfides are isotopic cousins to molybdenite. The acronym LLHR was introduced to describe 'low level' sulfides (ppb level Re and ppt level Os) which have 'highly radiogenic' Os isotopic compositions (Stein et al., 2000). Like molybdenite, on crystallization these sulfides have high Re/Os ratios ($^{187}Re/^{188}Os$ in the thousands) and minimal common or initial Os, although some is almost always present. Therefore, traditional $^{187}Re/^{188}Os$ versus $^{187}Os/^{188}Os$ isochron plots for data from LLHR samples should be employed with care. The risk is to plot ratios that are based on well-determined ^{187}Re and ^{187}Os concentrations that have been divided by imprecisely known or near zero ^{188}Os concentration (Stein et al., 2000). Isochron plots with $^{187}Re/^{188}Os$ ratios in the many hundreds of thousands are found in the literature today and should be evaluated carefully. The key piece of information in such a circumstance is assessment of the common Os concentration (i.e., ^{188}Os) – is it high enough to be well measured?

The effect of an increasing $^{187}Re/^{188}Os$ ratio on the observed present-day Os isotopic composition is illustrated in five pie diagrams, each representing a sample with 10 ppb Re, 120 million years of radiogenic Os ingrowth, and a starting Os isotopic composition of 0.1271 (Figure 9). The percentage of radiogenic ^{187}Os increases dramatically as $^{187}Re/^{188}Os$ increases toward molybdenite-like isotopic compositions where the component of radiogenic ^{187}Os becomes nearly 100% of the total Os (Figure 9). Some arsenopyrites (FeAsS) and pyrites (FeS$_2$) may be LLHR (Stein et al., 2000).

LLHR pyrite and arsenopyrite are particularly useful because these sulfides are common minerals in many ore deposits, from sedimentary-hosted to magmatic–hydrothermal ore environments. Further, nearly all of the world's Au deposits are associated with pyrite and/or arsenopyrite. LLHR compositions in these sulfides vastly widen the opportunity to date ore deposition directly in many different ore-forming environments. There is a caveat, however.

Like molybdenite, an initial Os isotopic ratio must be assumed for the age calculation; unlike molybdenite, this assumption matters. For example, an only moderately LLHR sample, in addition to a dose of common Os, may have only slightly high Re/Os ratios (e.g., $^{187}Re/^{188}Os$ $\sim$1000–2000). With this combination, selection of the initial $^{187}Os/^{188}Os$ ratio begins to impact the calculated age, and may reach the point where clarity of age fades; this lessens confidence in interpretation. Calculated ages for sulfides with only moderately LLHR compositions must be interpreted carefully, again calling for communication between those familiar with the geology and those performing the geochronology.

There are several possible reasons why some pyrites and arsenopyrites have LLHR compositions. Os in an ore-forming fluid may have taken residency in more chemically favorable coprecipitating sulfides or metal alloys leaving partner sulfides with much higher Re/Os ratios and creating their LLHR character. Alternatively, some ore-forming fluids may simply have inherently high Re/Os ratios. Low Os concentrations may be endemic to many crustally derived ore-forming fluids. However, ore-forming fluids entering, derived from, or passing through ultramafic rocks or clastic rocks with ultramafic detritus may acquire, deposit, and/or exchange Os with Os-bearing 'nuggets' that are far below visible detection. This process can greatly increase common Os in an ore system (see Section 13.4.6.1).

The first Re–Os study to combine Au-associated LLHR arsenopyrites with cogenetic pyrites of more 'normal' Os isotopic compositions netted a geologically significant 438 ± 6 Ma age for Au deposition at the Bendigo deposit in the Lachlan fold belt, southeastern Australia (Arne et al., 2001). The utility of LLHR sulfides has been demonstrated again and again. Gold-associated arsenopyrite was dated from the Maoling deposit in northeast China (Yu et al., 2005), the Puna region of northwest Argentina (Bierlein et al., 2006b), the Meguma terrane in Nova Scotia (Morelli et al., 2005), the renowned Homestake mine in South Dakota, USA (Morelli et al., 2010), and the giant Murantau Au deposit in Uzbekistan (Morelli et al., 2007). A bonus in working with only moderately LLHR samples is the acquisition of the initial $^{187}Os/^{188}Os$ ratio of the ore-forming fluid on an isochron plot. In the case of Bendigo, an initial $^{187}Os/^{188}Os$ ratio of 1.04 ± 0.16 clearly links Au to fluids in communication
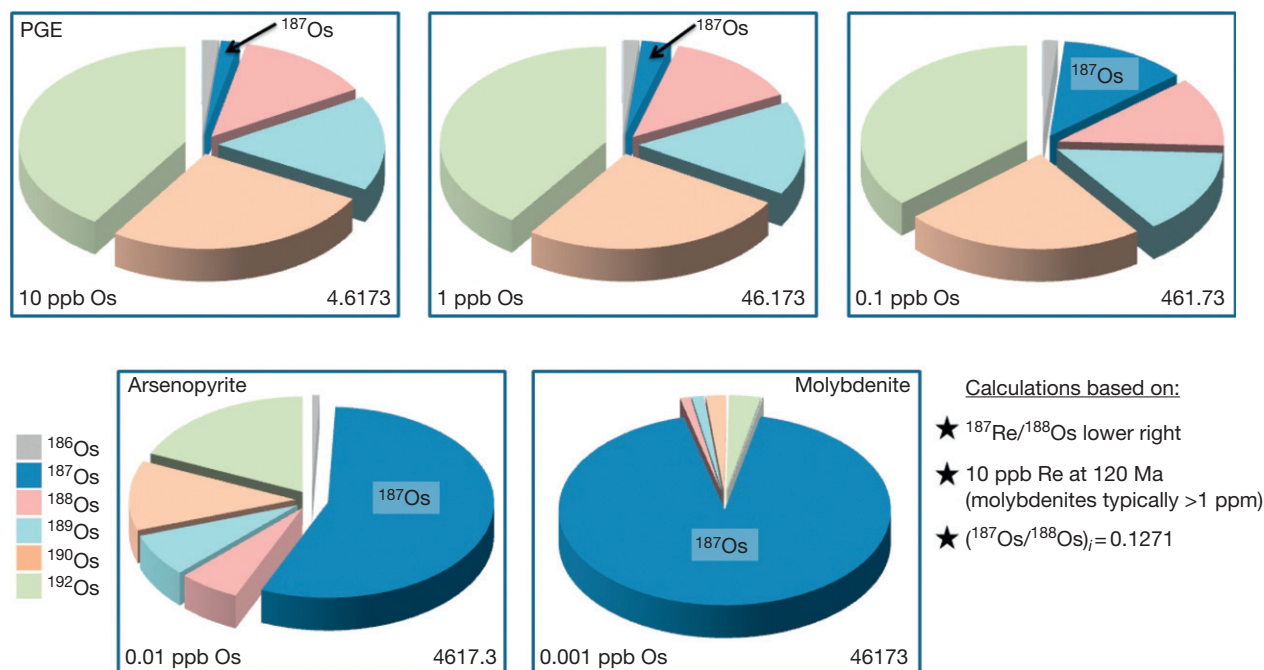
Figure 9   The effect of increasing $^{187}Re/^{188}Os$ ratio on the Os isotopic composition of a mineral after 120 m.y. of radiogenic ^{187}Os ingrowth assuming a starting $^{187}Os/^{188}Os$ isotopic composition of 0.1271 and 10 ppb Re. Note that ^{184}Os is not shown in legend as it is only 0.02% of total Os and would not form a visible slice of the pie. Low level highly radiogenic (LLHR) Os isotopic compositions (Stein et al., 2000) characterize some arsenopyrites. Molybdenites with low ppb level Re are extremely rare. For typical molybdenites with ppm level Re, the pie composition would appear completely blue (^{187}Os).

with average crustal rocks (e.g., hosting turbidites). In the case of Murantau, a mantle-like component was involved.

The field of Re–Os is still relatively new. There is no reference manual to suggest in advance if particular sulfides will have high Re/Os ratios. Molybdenite is nearly 100% certain to comply. Other sulfides have highly variable Re/Os ratios; for example, many chalcopyrites have low Re concentrations and low Re/Os ratios whereas in other examples they can be extraordinarily high. Selby et al (2009) report extreme LLHR examples of chalcopyrite, bornite and pyrite from a carbonate-hosted Cu deposit in the Brooks Range, Alaska. Prediction of Re and Os concentrations in ore minerals prior to analysis is based on understanding geologic setting and tectonic picture; these supply overriding information to predict Re and Os levels in general – the sulfides simply do their part in taking up these two elements.

13.4.6   Re–Os in Nonsulfides

Re and Os are chalcophile–siderophile elements and, like other metals, they have a high affinity for organic material (**Figure 1**). Os is more siderophile compared to Re which is strongly chalcophile. Both elements form sulfides and metal alloys. They do not form oxides. Both Re and Os are highly soluble under oxidizing conditions.

13.4.6.1   Chromite (FeCr$_2$O$_4$)

Platinum group minerals (PGM) are concentrated in Cr-spinel versus silicate fractions in the PGE environment. Experimental

studies suggest PGE form solid solutions in spinel (e.g., Capobianco et al., 1994; Park et al., 2012). Empirical observations, however, suggest that PGE are not structurally bound in Cr-spinels; rather, they are contained in sulfides and PGE metal alloys directly associated with chromitites (e.g., O'Driscoll et al., 2009). Conceptually, water-driven processes and melt percolation events over extended timescales in supra-subduction zones, essential to formation of podiform chromitite deposits (e.g., Matveev and Ballhaus, 2002; O'Driscoll et al., 2012), violate assumptions of same initial Os ratio as a starting point for geochronology (see **Section 13.4.3.2**). Documented variability in $^{187}Os/^{188}Os$ at the meter to micrometer scale in chromitite-associated PGE and base-metal sulfides reinforces the isotopic complexity associated with formation of chromite ores (e.g., González-Jiménez et al., 2012a; Marchesi et al., 2011). Mobility of Re and Os in PGM in chromitites during metamorphism is also recorded in Os isotopic compositions (González-Jiménez et al., 2012b).

While disturbance of Os isotope systematics in podiform chromitite is in itself an important phenomenon, chromite (and/or its PGM mineral inclusions and rims) is not suitable for Re–Os geochronology because its Re/Os ratios are extremely low. It is impossible to precisely measure ^{187}Os daughter from radioactive decay when there is almost no Re present (<10 ppt) and significant common Os is present. For chromites, $^{187}Re/^{188}Os$ ratios as low as 0.00113 ± 0.00008 have been measured (Shi et al., 2012b); $^{187}Re/^{188}Os$ are typically <0.1.

A deeper understanding of serpentinization and deserpentinization processes in harzburgites and dunites is essential to understanding chromitites and their sulfides, arsenides and PGM. Ultimately, robust geochronology at crustal levels

requires processes that homogenize (erase) any heterogeneity developed in mantle rocks.

13.4.6.2 Magnetite (Fe$_3$O$_4$)

Compared to chromite, magnetite is abundantly present in many ore deposits. Notably, it is ubiquitous in porphyry Cu–Au–Mo and porphyry Mo deposits worldwide. In porphyry-style deposits, magnetite usually forms early in the paragenesis, signaling moderately oxidizing preore conditions. Re–Os data for magnetite are limited, in part because many magnetite-bearing deposits in the porphyry environment contain readily datable molybdenite for precise and accurate age information. For some IOCG deposits where magnetite–hematite is an economic commodity, molybdenite is also available to establish the age of the IOCG mineralization (Skirrow et al., 2007). In doing so, it is important that the contemporaneity of magnetite and molybdenite is well established in the field.

Re–Os data for titanomagnetite are reported from the intertwined Fe–Ti–V oxide and Fe–Cu–Ni sulfide deposits in the Suwalki anorthosite massif, NE Poland (Morgan et al., 2000). Compared to Re and Os concentrations in coprecipitating sulfide, the titanomagnetites register an order of magnitude lower concentrations. Variation in Re and Os concentrations for magnetites is attributed to sub-mm to micron-size sulfide inclusions, unavoidable during mechanical separation of mineral phases. The ^{187}Re/^{188}Os ratios for magnetites, therefore, present maximum values, with corresponding sulfide phases containing much higher ^{187}Re/^{188}Os.

Similarly, Re–Os data for magnetite-rich samples from the Biwabik banded iron formation, Minnesota, show low concentrations of both Re (<2 ppb) and Os (<30 ppb), with consistently low Re/Os ratios (<7; Ripley et al., 2008). As with chromitites, the iron oxide phases are useful for Os tracer studies, but not geochronology.

In a Re–Os study of magnetite–pyrite sample pairs from the Cala IOCG mine in the Ossa Morena Zone of SW Iberia, pyrite is clearly observed postdating magnetite. Pyrite veinlets engulf and penetrate massive brecciated magnetite. A 7-point magnetite–pyrite Re–Os isochron suggests a sudden change in oxidation state at the Frasnian–Famennian boundary without significant change in the Re and Os concentrations in the fluid (Carriedo et al., 2007; Stein et al., 2006).

13.4.6.3 Native Gold

Limited studies of Re–Os systematics in native gold consistently show blank level concentrations of Re and low, but more variable concentrations of Os. Analyses of two lots of gold wire at the AIRIE Program, Colorado State University (unpublished data) and a gold coin and gold powder at the University of Arizona (Kirk et al., 1998) yielded blank level Re concentrations and <150 ppt Os. Archean gold samples from the Yilgarn (Chalice mine) and Abitibi (Sigma mine) yield <20 ppt Re and <50 ppt Os, but two gold samples from the Mesozoic El Tierrero deposit, Nambija district, southern Ecuador yield precise concentrations of 90 and 119 ppt Re and 0.52 and 1.2 ppb Os, with a consistent initial ^{187}Os/^{188}Os ratio of 0.53 ± 0.05 (Hannah et al., 2004b). Kirk et al. (2002) plot data fields (actual data not tabulated) for gold from Gympie

(Queensland, Australia), Moeda (Minas Gerais, Brazil), and a Papua New Guinea epithermal deposit, for which Os ranges from <10 to ~300 ppt (most <50 ppt), and Re ranges from 2 ppt to ~8 ppb. In almost every case, Re and Os concentrations approach blank levels, and low Re/Os ratios preclude use of native gold as a geochronometer.

If native Au contained Re and Os, the Witwatersrand gold deposits are an obvious target for geochronology, given a century of controversy over their origin. Kirk et al. (2002) asserted a ~3 Ga age for the gold, and hence, a detrital origin, based on Re–Os analyses of five splits of gold separated from a single hand sample. *But the apparent isochron is based almost entirely on variations in Os alone.* Re concentrations range only from 2.5 to 11.4 ppb, while Os ranges from 4 to 4162 ppb – over three orders of magnitude. This is a classic example of the nugget effect, in which Os concentrations vary because of variable microinclusions of osmiridium, an OsIr alloy known to occur in the Witwatersrand sedimentary rocks. The highest measured concentration of Os is readily explained by a 5-µm diameter inclusion of osmiridium in a 1 mm^3 grain of gold, and thus, almost impossible to capture microscopically. This interpretation is further supported by data for gravity concentrates from the Western Areas mill reported in Kirk et al. (2001). Os ranges from 6989 to 10 350 ppb in bulk samples of gold ore, but drops to 224–1387 ppb in hand-picked gold from the same concentrates. Clearly there is a high-Os mineral – most likely osmiridium – accompanying the gold in the concentrates, and present within hand-picked gold grains (Hannah et al., 2004b). In sum, native gold seems to be a poor candidate for Re–Os geochronology, but may provide constraints on initial ^{187}Os/^{188}Os ratios in cases where measured Os can be attributed with certainty to the gold itself rather than exotic microinclusions.

13.4.7 A Clock for Metal Release and Migration from Hydrocarbon Maturation

Black shales are a major repository of metals in Earth's crust (Figure 1). Organic-rich sediments deposited under anoxic conditions have been highly effective at sequestering metals from seawater and lacustrine systems throughout Earth history. Therefore, organic-rich rocks with high Re and Os concentrations provide the possibility to date the sedimentary rock record. The isochron approach provides the initial Os isotopic composition, a telling recorder of the paleoenvironment and the fluids that equilibrated with organic-rich sedimentation. Maturation and migration of hydrocarbon creates its own new clock. The initial Os ratio in migrated hydrocarbon places constraints on source rock for that hydrocarbon. Much like the drop in the ocean analogy presented in Section 13.4.3.2.3.2, the clock in the source rock is generally maintained during this process. This remarkable phenomenon brings the dimension of absolute time to petroleum geology.

Visible and microscale organic material in sedimentary-hosted ore deposits is common, though its presence is generally a footnote to the sulfide mineralization. It may occur as conspicuously as veinlets and breccia-fill or as subtly as a component of fluid inclusions or calcite cements (e.g., Ettner et al., 1996; Hollis, 1998; Parnell, 1994; Parnell and

Swainbank, 1990; Pfaff et al., 2010; Rickard et al., 1975), and it may be present as detrital grains of kerogen. In particular, hydrocarbon has been a controversial player in the renowned Au deposits at Witwatersrand, South Africa (e.g., Fuchs et al., 2011; see also Section 13.4.6.3). The consistent spatial and paragenetic association of gold with 'hydrocarbon leaders' logically suggests that metals and hydrocarbon might have had the same source, or that they may have traveled together in the same fluid. Kerogens, the precursor to hydrocarbons, are metal-rich and characteristically have Re and Os at the ppb level (e.g., Creaser et al., 2002; Georgiev et al., 2011; Ravizza and Turekian, 1989; Xu et al., 2009). Heating or oxidation of organic-rich sequences leads to breakdown of organic material and consequently, release of significant quantities of metal. Add fluid (H_2O, CH_4, and/or CO_2) and a physical–chemical gradient, and the metals (and hydrocarbon) will migrate. *Logic dictates that the maturation and migration of hydrocarbon must be intimately associated with the release and/or migration of metals.*

The concept is simple. If migrated hydrocarbon is dated, the timing of associated metal migration and subsequent sulfide deposition is constrained. Metal-bearing fluids traveling with hydrocarbon, however, may forfeit Re and Os to the hydrocarbon rather than incorporating these elements into sulfide on ore deposition. The distribution of Re and Os among sulfide and hydrocarbon phases will be different for different deposits, and will vary along migration paths.

At the Red Dog Zn–Pb–Ag deposit in the Brooks Range, Alaska, pyrite and presumed cogenetic sphalerite have quite different Re–Os characteristics; pyrite has relatively high Re–Os concentrations, high Re/Os ratios and is isochronous, whereas sphalerite, has much lower Re–Os concentrations, low Re/Os ratios, and is not isochronous (Morelli et al., 2004). This outcome is attributed to postdepositional disturbance affecting only sphalerite (Morelli et al., 2004). Alternatively, the sphalerite disturbance may not have been postdepositional. The disturbance may have resulted from interaction with hydrocarbons during metal transport and/or deposition (Warner, 1998). Chemical or isotopic exchange with Re–Os-rich hydrocarbons could easily produce variations in the initial $^{187}Os/^{188}Os$ ratio in sphalerite because of its low Os concentrations. Further, the modest range in $^{187}Re/^{188}Os$ in the Red Dog sphalerites combined with any initial $^{187}Os/^{188}Os$ variation magnifies the uncertainty on the age. The result is non-isochronous behavior. The pyrite, in contrast, is less affected by interaction with hydrocarbon because it has much higher starting Os concentrations. Also, the extreme variation in $^{187}Re/^{188}Os$ (up to 5000) and LLHR character of some pyrites permit a relatively precise age (338.3 ± 5.8, Model 3; Morelli et al., 2004), covering up small to moderate variations in initial $^{187}Os/^{188}Os$. Although the pyrite age is useful, the initial Os ratio given by the isochron has a high uncertainty (0.20 ± 0.21), and the isochron MSWD of 7.8 suggests real geologic variation in the initial Os isotopic ratio. That is why a Model 3 age is generated (see Section 13.4.3.2.2).

A reverse logic can be applied. That is, knowing the age of an ore deposit, Re–Os data from ore-associated organic material can be used to reproduce that age (e.g., Christensen et al., 1995b; Selby et al., 2005). Also, Re–Os data place limits on the source rock for ore-forming fluids. As an example, the age for the renowned Eocene Carlin Au deposits has long been controversial, though a Rb–Sr age on galkhaite, a mercury sulfosalt, suggests ∼40 Ma (e.g., Muntean et al., 2011; Tretbar et al., 2000). Gold (electrum) and sulfide minerals (orpiment and realgar) have Re and Os levels that are too low to provide age information and the magnitude of the blank correction prohibits definitive information on the initial $^{187}Os/^{188}Os$ ratio (Hofstra and Creaser, 2009; Hofstra et al., 1999). Gold-associated arsenian pyrite is very fine grained and characteristically shows multiple overgrowths; since Re–Os dating is performed on mechanically derived mineral separate, micron-scale overgrowths are prohibitive.

Re–Os analyses of bitumen from the Carlin district yield generous concentrations of Re and Os, but the Os is dominated by common Os (Figure 10). This can be turned to our advantage, as the isotopic composition of common Os reveals fluid source, and the geologically young age of mineralization at Carlin gives little time for ingrowth of radiogenic ^{187}Os. To accommodate the measured $^{187}Os/^{188}Os$ in the two hydrocarbon samples (Carlin and Blue Dick mines), the initial Os ratios 40 million years ago must be between 2.0 and 2.8. If the Os were derived directly from mafic rocks, its initial ratio would be less than 0.2. Therefore, the Os in the Au-associated hydrocarbon could not simply have come from a primitive source. Is it logical to argue that the Os in the Au-bearing sulfides came from a completely different source than the Os in the paragenetically intertwined hydrocarbon? Probably not. What kind of source rocks might provide $^{187}Os/^{188}Os$ ratios of 2.0–2.8 to the ore–hydrocarbon fluids? Marine black shales from the Upper Devonian Exshaw Formation in Alberta, dated by Re–Os at 358 ± 9 Ma, have present-day $^{187}Os/^{188}Os$ ratios that range from about 1.8 to 4.0 (Creaser et al., 2002). A time correlative marine margin along western North America includes marine shales of similar age, known to underlie the Carlin region in Nevada. The Os budget in bitumen from the Au ore zone in the Carlin region could be fully accommodated by an Os source from Upper Devonian black shales. This scenario does not exclude other components in the ore fluid or limit the ore-forming process, but the radiogenic Os isotopic composition of bitumen entwined with Au ore must be accounted for in any ore deposit modeling. For the Carlin district, that will be hard to do without including shale in the ore-forming equation.

13.4.8   Future of Dating for Ore Geology and Mineral Exploration

The coming decades will merge vast archives of descriptive information for ore deposits with studies carrying the time component. Integration of information from disciplines outside the traditional boundaries of economic geology will be increasingly important. The timing of processes that move hydrocarbon is critically important to the timing of processes that move metal through the crust. Development of new ideas in economic geology will take advantage of studies in fluid, metal, and hydrocarbon mobility. A refined timing of key tectonic relationships that move metals through the crust will be important to defining prospective new regions. Expertise in geodynamics and the assembly and dismemberment of paleocontinents through time will be in demand. This will enable

Re–Os data for two samples of bitumen associated with Au ore from the Carlin Au region, Nevada, USA

AIRIE Run #	Locality	Re (ppb)	Total Os (ppb)	Common Os (ppb)	$^{187}Re/^{188}Os$	$^{187}Os/^{188}Os$	$^{187}Os/^{188}Os_i$ to achieve $^{187}Os/^{188}Os_m$
ORG-248	Blue Dick Mine	39.80 (2)	0.389 (3)	0.373	639 (1)	2.408 (5)	2.00
ORG-249	Carlin Mine	20.88 (1)	0.624 (4)	0.614	219.8 (4)	2.905 (6)	2.75

Carius tube dissolution and equilibration with single Re and Os spikes; sample weights 213 and 267 mg for ORG-248 and ORG-249, respectively
Analyses by NTIMS, AIRIE Program-CSU; Data are blank-corrected for Re = 12.7 ± 0.2 pg, Os = 0.115 ± 0.001 pg with $^{187}Os/^{188}Os = 0.228 ± 0.003$
Initial (i) $^{187}Os/^{188}Os$ calculation based on 40 Ma assumed age for Carlin Au mineralization; Measured (m) is present day $^{187}Os/^{188}Os$
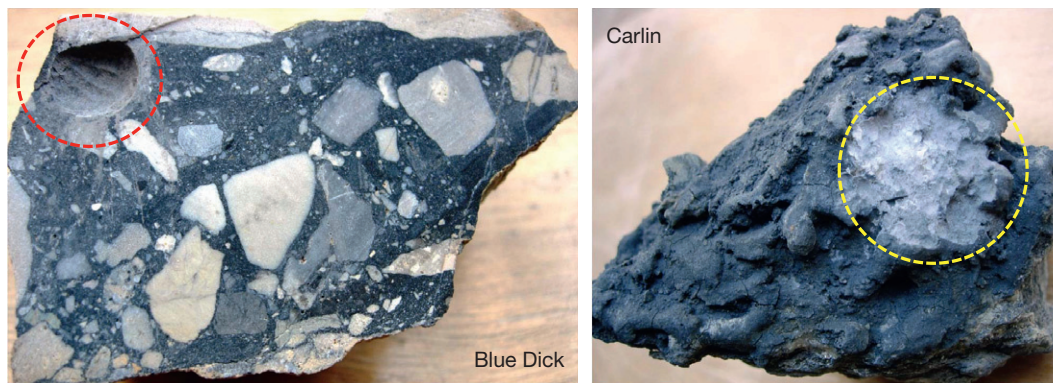
Figure 10 Re–Os characteristics for two samples of Au ore containing bitumen from the Carlin Au region, Nevada, USA. Blue Dick sample is a polylithic breccia cemented by hydrocarbon-rich matrix; drill pit outlined in red dashed circle is about 1 cm across and shows excavated hydrocarbon-rich matrix. Carlin sample is hydrocarbon in open-space coating brecciated host rock; drilled surface outlined in dashed yellow circle about 2 cm across shows hydrocarbon-rich separate. Discussion in text.

exploration to advance in new ways. While prospecting in existing mineral belts will remain important, the larger advances will be made through better linkage of plate margin and craton interior dynamics. Recognition of terranes with shared geologic and tectonic histories will increase exploration success. Timing of metal-releasing and metal-arresting events at the global scale will underpin new advances in ore geology. Widespread oxidation events in solid earth need better documentation and explanation. Winning companies will thrive on the creativity of geoscientists from unlikely backgrounds who examine metal mobility and sulfide deposition from very different vantages. In turn, those working to resolve large questions in Earth, atmosphere, and seawater evolution will thrive on the contributions of creative ore geologists.

References

Aleinikoff JN, Creaser RA, Lowers HA, Magee CW, and Grauch RI (2012) Multiple age components in individual molybdenite grains. *Chemical Geology* 300–301: 55–60.

Alexandre P, Kyser K, Jiricka D, and Witt G (2012) Formation and evolution of the Centennial unconformity-related uranium deposit in the south-central Athabasca basin, Canada. *Economic Geology* 107: 385–400.

Allaz J, Engi M, Berger A, and Villa IM (2011) The effects of retrograde reactions and of diffusion on $^{40}Ar–^{39}Ar$ ages of micas. *Journal of Petrology* 52: 691–716.

Anglin CD, Johasson IR, and Franklin JM (1996) Sm–Nd dating of scheelite and tourmaline: Implications for the genesis of Archean gold deposits, Val d'Or, Canada. *Economic Geology* 91: 1372–1382.

Arne D, Bierlein F, Morgan JW, and Stein HJ (2001) Re–Os dating of sulfides associated with gold mineralization in central Victoria, Australia. *Economic Geology* 96: 1455–1459.

Arribas A, Arribas I, Draper G, et al. (2011) ^{40}Ar/^{39}Ar dating of alunite from the Pueblo Viejo gold–silver district, Dominican Republic. *Economic Geology* 106: 1059–1070.

Atkinson WW Jr., Souviron A, Vehrs TI, and Faunes A (1996) Geology and mineral zoning of the Los pelambres porphyry copper deposit, Chile. *Society of Economic Geologists Special Publication* 5: 131–156.

Barra F, Ruiz J, Mathur R, and Titley S (2003) A Re–Os study of sulfide minerals from the Bagdad porphyry Cu–Mo deposit, northern Arizona, USA. *Mineralium Deposita* 38: 585–596.

Beard JS (2008) Crystal-melt separation and the development of isotopic heterogeneities in hybrid magmas. *Journal of Petrology* 49: 1027–1041.

Beard JS, Ragland PC, and Crawford ML (2005) Reactive bulk assimilation: A model for crust-mantle mixing in silicic magmas. *Geology* 33: 681–684.

Bekker A, Holland HD, Wang P-L, et al. (2004) Dating the rise of atmospheric oxygen. *Nature* 427: 117–120.

Bell K, Anglin CD, and Franklin JM (1989) Sm–Nd and Rb–Sr isotope systematics of scheelites: Possible implications for the age and genesis of vein-hosted gold deposits. *Geology* 17: 500–504.

Bergemann F, Ludwig KR, Lugmair GW, et al. (2001) Call for an improved set of decay constants for geochronological use. *Geochimica et Cosmochimica Acta* 65: 111–121.

Bierlein FP, Groves DI, Goldfarb RJ, and Dubé B (2006a) Lithospheric controls on the formation of provinces hosting giant orogenic gold deposits. *Mineralium Deposita* 40: 874–886.

Bierlein FP, Stein HJ, Coira B, and Reynolds P (2006b) Timing of gold and crustal evolution of the Paleozoic south central Andes, NW Argentina – Implications for the endowment of orogenic belts. *Earth and Planetary Science Letters* 245: 702–721.

Bingen B and Stein H (2003) Molybdenite Re–Os dating of biotite dehydration melting in the Rogaland high-temperature granulites, S Norway. *Earth and Planetary Science Letters* 208: 181–195.

Bingen B, Stein HJ, Bogaerts M, Bolle O, and Mansfeld J (2006) Molybdenite Re–Os dating constrains gravitational collapse of the Sveconorwegian orogen, SW Scandinavia. *Lithos* 87: 328–346.

Brannon JC, Podosek FA, and McLimans RK (1992) Alleghenian age of the upper Mississippi Valley zinc–lead deposit determined by Rb–Sr dating of sphalerite. *Nature* 356: 509–511.

Braxton DP, Cooke DR, Dunlap J, et al. (2012) From crucible to graben in 2.3 Ma: A high-resolution geochronological study of porphyry life cycles, Boyongan–Bayugo copper–gold deposits, Phillippines. *Geology* 40: 471–474.

Brenan JM, Cherniak DJ, and Rose LA (2000) Diffusion of osmium in pyrrhotite and pyrite: Implications for closure of the Re–Os isotopic system. *Earth and Planetary Science Letters* 180: 399–413.

Cannell J, Cooke DR, Walshe JL, and Stein H (2005) Geology, mineralization, alteration, and structural evolution of the El Teniente porphyry Cu–Mo deposit. *Economic Geology* 100: 979–1003.

Capobianco CJ, Hervig RL, and Drake MJ (1994) Experiments on crystal/liquid partitioning of Ru, Rh and Pd for magnetite and hematite solid solutions crystallized from silicate melt. *Chemical Geology* 113: 23–43.

Carriedo J, Tornos F, Velasco F, and Stein H (2007) Complex structural and hydrothermal evolution of the Cala magnetite deposit, SW Iberia – An ICOG deposit? In: Andrews CJ, et al. (ed.) *Digging Deeper*, vol. 2, pp. 1351–1354. Dublin: Irish Association for Economic Geology.

Cathles LM, Erendi AHJ, and Barrie T (1997) How long can a hydrothermal system be sustained by a single intrusive event? *Economic Geology* 92: 766–771.

Cathles LM and Shannon R (2007) How potassium silicate alteration suggests the formation of porphyry copper deposits begins with the nearly explosive but barren expulsion of large volumes of magmatic water. *Earth and Planetary Science Letters* 262: 92–108.

Chamberlain KR, Schmitt AK, Swapp SM, et al. (2010) In situ U–Pb SIMS (IN–SIMS) micro-baddeleyite dating of mafic rocks: Method with examples. *Precambrian Research* 183: 379–387.

Chesley JT, Halliday AN, Kyser TK, and Spry PG (1994) Direct dating of Mississippi Valley-type mineralization: Use of Sm–Nd in fluorite. *Economic Geology* 89: 1192–1199.

Christensen JN, Halliday AN, Leigh KE, Randell RN, and Kesler SE (1995a) Direct dating of sulfides by Rb–Sr: A critical test using the Polaris Mississippi Valley-type Zn–Pb deposit. *Geochimica et Cosmochimica Acta* 59: 5191–5197.

Christensen JN, Halliday AN, Vearncombe JR, and Kesler SE (1995b) Testing models of large-scale crustal fluid flow using direct dating of sulfides: Rb–Sr evidence for early dewatering and formation of Mississippi Valley-type deposits, Canning Basin, Australia. *Economic Geology* 90: 877–884.

Coggon JA, Nowell GM, Pearson DG, Lorand J-P, Oberthür T, and Parman SW (2010) Dating platinum mineralization using the ^{190}Pt–^{186}Os system: Examples from the Bushveld complex, RSA and the Meratus ophioite, Borneo. In: *11th International Platinum Symposium, Ontario Geological Survey, Miscellaneous Release – Data 269*, p 4.

Cohen AS and Waters FG (1996) Separation of osmium from geological materials by solvent extraction for analysis by thermal ionization mass spectrometry. *Analytica Chimica Acta* 332: 269–275.

Colodner D, Sachs J, Ravizza G, Turekian K, Edmond J, and Boyle E (1993) The geochemical cycle of rhenium: A reconnaissance. *Earth and Planetary Science Letters* 117: 205–221.

Corfu F, Hanchar JM, Hoskin PWO, and Kinny PD (2003) Atlas of zircon textures. In: Hancher JM and Hoskin PWO (eds.) *Zircon*, vol. 53, pp. 469–500. Washington, DC: Reviews in Mineralogy and Geochemistry.

Cornell DH, Pettersson Å, Whitehouse MJ, and Scherstén A (2009) A new chronostratigraphic paradigm for the age and tectonic history of the Mesoproterozoic Bushmanland ore district, South Africa. *Economic Geology* 104: 385–404.

Creaser RA, Papanastassiou DA, and Wasserburg GJ (1991) Negative thermal ion mass spectrometry of osmium, rhenium and iridium. *Geochimica et Cosmochimica Acta* 55: 397–401.

Creaser RA, Sannigrahi P, Chacko T, and Selby D (2002) Further evaluation of the Re–Os geochronometer in organic-rich sedimentary rocks: A test of hydrocarbon maturation effects in the Exshaw Formation, Western Canada Sedimentary Basin. *Geochimica et Cosmochimica Acta* 66: 3441–3452.

Cumming GL and Richards JR (1975) Ore lead isotope ratios in a continuously changing earth. *Earth and Planetary Science Letters* 28: 155–171.

Darbyshire DPF, Pitfield PEJ, and Campbell SDG (1996) Late Archean and Early Proterozoic gold–tungsten mineralization in the Zimbabwe Archean craton: Rb–Sr and Sm–Nd isotope constraints. *Geology* 24: 19–22.

Davidson JP, Morgan DJ, Charlier BLA, Harlou R, and Hora JM (2007) Microsampling and isotopic analysis of igneous rocks: Implications for the study of magmatic systems. *Annual Review of Earth and Planetary Sciences* 35: 273–311.

Demaiffe D, Wiszniewska J, Krzemińska E, et al. (2013) A hidden alkaline and carbonatite province of early carboniferous age in northeast Poland: Zircon U–Pb and pyrrhotite Re–Os geochronology. *Journal of Geology* 121: 91–104.

Dempster TJ, Martin JC, and Shipton ZK (2008) Zircon dissolution in a ductile shear zone, Monte Rosa granite gneiss, northern Italy. *Mineralogical Magazine* 72: 971–986.

Du A, He H, Yin N, et al. (1995) A study of the rhenium–osmium geochronometry of molybdenite (in English). *Acta Geologica Sinica* 8: 171–181.

Du A, Wu S, Sun D, et al. (2004) Preparation and certification of Re–Os dating reference materials: Molybdenites HLP and JDC. *Geostandards and Geoanalytical Research* 28: 41–52.

Eichhorn RE, Höll R, Jagoutz E, and Schärer U (1997) Dating scheelite stages: A strontium, neodymium, lead approach from the Felbertal tungsten deposit, central Alps, Austria. *Geochimica et Cosmochimica Acta* 61: 5005–5022.

Eikenberg J and Köppel V (1995) Application of U–Xe and U–Kr systems for dating U minerals: A key for interpreting discordant U–Pb ages. *Chemical Geology (Isotope Geoscience Section)* 123: 209–223.

Emmons SF (1904) Theories of ore deposition, historically considered. *Geological Society of America* 15: 1–28.

Ettner DC, Lindblom S, and Karlsen D (1996) Identification and implications of light hydrocarbon fluid inclusions from the Proterozoic Bidjovagge gold–copper deposit, Finnmark, Norway. *Applied Geochemistry* 11: 745–755.

Faure G and Mensing TM (2005) *Isotopes: Principles and Applications*, 3rd ed. Hoboken, NJ: Wiley, p 896.

Flowers RM, Schmitt AK, and Groves M (2010) Decoupling of U–Pb dates from chemical and crystallographic domains in granulite facies zircon. *Chemical Geology* 270: 20–30.

Förster H-J, Rhede D, Stein HJ, Romer RL, and Tischendorf G (2012) Paired uraninite and molybdenite dating of the Königshain granite; implications for the onset of late-Variscan magmatism in the Lausitz Block. *International Journal of Earth Sciences* 101: 57–67.

Frei R, Dahl PS, Frandsson MM, et al. (2009) Lead-isotope and trace-element geochemistry of Paleoproterozoic metasedimentary rocks in the Lead and Rochford basins (Black Hills, South Dakota, USA): Implications for genetic models, mineralization ages, and sources of leads in the Homestake gold deposit. *Precambrian Research* 172: 1–24.

Frei R, Nägler ThF, Schönberg R, and Kramers JD (1998) Re–Os, Sm–Nd, U–Pb, and stepwise lead leaching isotope systematics in shear-zone hosted gold mineralization: Genetic tracing and age constraints of crustal hydrothermal activity. *Geochimica et Cosmochimica Acta* 62: 1925–1936.

Frei R and Pettke T (1996) Mono-sample Pb-Pb dating of pyrrhotite and tourmaline: Proterozoic vs. Archean intracratonic gold mineralization in Zimbabwe. *Geology* 24: 823–826.

Fuchs S, Kloess G, and Williams-Jones A (2011) Petroleum as a potential agent for gold transport and deposition in the Black Reef Formation, South Africa. *'Let's Talk Ore Deposits,' Proceedings of the Eleventh Biennial SGA Meeting* 586–588.

Geisler T, Schaltegger U, and Tomaschek F (2007) Zircon tiny but timely. Re-equilibration of zircon in aqueous fluids and melts. *Elements* 3: 43–50.

Georgiev S, Stein HJ, Hannah JL, Bingen B, Weiss HM, and Piasecki S (2011) Hot acidic late Permian seas stifle life in record time. *Earth and Planetary Science Letters* 310: 389–400.

Georgiev S, Stein HJ, Hannah JL, et al. (2012) Geochemistry of Arctic black shales and the effect of weathering on Re–Os isotope systematics. *Chemical Geology* 324–325: 108–121.

Glazner AF (2007) Thermal limitations on incorporation of wall rock into magma. *Geology* 35: 319–322.

Glodny J and Grauert B (2009) Evolution of a hydrothermal fluid–rock interaction system as recorded by Sr isotopes: A case study from the Schwarzwald, SW Germany. *Mineralogy and Petrology* 95: 163–178.

Glodny J, Kühn A, and Austrheim H (2008) Geochronology of fluid-induced eclogite and amphibolite facies metamorphic reactions in a subduction-collision system, Bergen Arcs, Norway. *Contributions to Mineralogy and Petrology* 156: 27–48.

González-Jiménez JM, Gervilla F, Griffin WL, et al. (2012a) Os-isotope variability within sulfides from podiform chromitites. *Chemical Geology* 291: 224–235.

González-Jiménez JM, Griffin WL, Gervilla F, et al. (2012b) Metamorphism disturbs the Re–Os signatures of platinum-group minerals in ophiolite chromitites. *Geology* 40: 659–662.

Graton LC (1941) Ore Deposits. *Geological Society of America* Fiftieth Anniversary Volume, 471–509.

Groves DI, Bierlein FP, Meinert LD, and Hitzman MW (2010) Iron oxide copper-gold (IOCG) deposits through earth history: Implications for origin, lithospheric setting, and distinction from other epigenetic iron oxide deposits. *Economic Geology* 105: 641–654.

Gustavson LB and Hunt JP (1975) The porphyry Cu deposit at El Salvador, Chile. *Economic Geology* 70: 857–912.

Hannah JL, Bekker A, Stein HJ, Markey RJ, and Holland HD (2004a) Primitive Os and 2316 Ma age for marine shale: Implications for Paleoproterozoic glacial events and the rise of atmospheric oxygen. *Earth and Planetary Science Letters* 225: 43–52.

Hannah JL, Stein HJ, Markey RJ, and Scherstén A (2004b) Gold: A Re–Os geochronometer? *Geochimica et Cosmochimica Acta* 68: A773.

Hannah JL, Stein HJ, Wieser ME, de Laeter JR, and Varner M (2007) Mo isotope variations in molybdenite: Vapor transport and Rayleigh fractionation of Mo. *Geology* 35: 703–706.

Harlov DE, Wirth R, and Hetherington CJ (2011) Fluid-mediated partial alteration in monazite: The role of coupled dissolution–reprecipitation in element redistribution and mass transfer. *Contributions to Mineralogy and Petrology* 162: 329–348.

Harris AC and Golding SD (2002) New evidence of magmatic-fluid-related phyllic alteration: Implications for the genesis of porphyry Cu deposits. *Geology* 30: 335–338.

Harrison TM and Zeitler PK (2005) Fundamentals of noble gas thermochronology. *Reviews in Mineralogy and Geochemistry* 58: 123–149.

Hehnke C, Ballantyne G, Martin H, Hart W, Schwarz A, and Stein H (2012) Geology and exploration progress at the resolution porphyry Cu–Mo deposit, Arizona. Society of Economic Geologists: Special Publication 16, pp. 147–166.

Herr W and Merz E (1955) Eine neue Methode zur Alterbestimmung von Rhenium-Haltigen Mineralien Mittels Neutronaktivierung. *Zeitschrift für Naturforschung. Part A – Astrophysik, Physik und Physikalische Chemie* 10: 613–615.

Herr W, Wölfle EP, and Kopp E (1967) Development and recent applications of the Re/Os dating method. In: *Radioactive Dating and Methods of Low-Level Counting*, pp. 499–508. Vienna: International Atomic Energy Agency.

Hiess J, Condon DJ, McLean N, and Noble SR (2012) $^{238}U/^{235}U$ systematics in terrestrial uranium-bearing minerals. *Science* 335: 1610–1614.

Hirt B, Herr W, and Hoffmeister W (1963) Age determinations by the rhenium-osmium method. In: *Radioactive Dating*, pp. 35–43. Vienna: International Atomic Energy Agency.

Hofstra AH and Creaser RA (2009) Re–Os isotope results for electrum from three low sulfidation epithermal Au–Ag deposits in the Great Basin. *Geological Society of America Abstracts with Programs* 41: 20.

Hofstra AH, Snee LW, Rye RO, et al. (1999) Age constraints on Jerritt Canyon and other Carlin-type gold deposits in the western United States – Relationship to mid-Tertiary extension and magmatism. *Economic Geology* 94: 769–802.

Hollis C (1998) Reconstructing fluid history: An integrated approach to timing fluid expulsion and migration on the Carboniferous Derbyshire Platform, England. In: Parnell J (ed.) *Dating and Duration of Fluid Flow and Fluid–Rock Interaction*, vol. 144, pp. 153–159. London: Geological Society Special Publications.

Jahn B-M and Cuvellier H (1994) Pb–Pb and U–Pb geochronology of carbonate rocks: An assessment. *Chemical Geology* 115: 125–151.

Jamtveit B and Hammer Ø (2012) Sculpting of rocks by reactive fluids. *Geochemical Perspectives* 1: 341–480.

Jiang Y-D, Qiu H-N, and Xu Y-G (2012) Hydrothermal fluids, argon isotopes and mineralization ages of the Fankou Pb–Zn deposit in south China: Insights from sphalerite $^{40}Ar/^{39}Ar$ progressive crushing. *Geochimica et Cosmochimica Acta* 84: 369–379.

Kempe U, Belyatsky BV, Krymsky RS, Kremenetsky AA, and Ivanov PA (2001) Sm–Nd and Sr isotope systematics of scheelite from the giant Au(–W) deposit Muruntau (Uzbekistan): Implications for the age and source of the Au mineralization. *Mineralium Deposita* 36: 379–392.

Kendrick MA, Miller J McL, and Phillips D (2006) Part II. Evaluation of $^{40}Ar–^{39}Ar$ quartz ages: Implications for fluid inclusion retentivity and determination of initial $^{40}Ar/^{36}Ar$ values in Proterozoic samples. *Geochimica et Cosmochimica Acta* 70: 2562–2576.

Kent AJR, Campbell IH, and McCulloch MT (1995) Sm–Nd systematics of hydrothermal scheelite from the Mount Charlotte mine, Kalgoorlie, Western Australia: An isotopic link between gold mineralization and komatiites. *Economic Geology* 90: 2329–2335.

Kirk J, Ruiz J, Chesley J, and Titley SR (1998) Re–Os systematics of gold. *Geological Society of America Abstracts with Programs* 30: 83.

Kirk J, Ruiz J, Chesley J, Titley S, and Walshe J (2001) A detrital model for the origin of gold and sulfides in the Witwatersrand basin based on Re–Os isotopes. *Geochimica et Cosmochimica Acta* 65: 2149.

Kirk J, Ruiz J, Chesley J, Walshe J, and England G (2002) A major Archaean, gold- and crust-forming event in the Kaapvaal craton, South Africa. *Science* 297: 1856–1858.

Kohn MJ and Vervoort JD (2008) U–Th–Pb dating of monazite by single-collector ICP-MS: Pitfalls and potential. *Geochemistry, Geophysics, Geosystems* 9: 16 Q04031.

Košler J, Simonetti A, Sylvester PJ, Cox RA, Tubrett MN, and Wilton DC (2003) Laser-ablation ICP-MS measurements of Re/Os in molybdenite and implications for Re–Os geochronology. *The Canadian Mineralogist* 41: 307–320.

Kusiak MA, Dunkley DJ, Słaby E, Martin H, and Budzyń B (2009) Sensitive high-resolution ion microprobe analysis of zircon reequilibrated by late magmatic fluids in a hybridized pluton. *Geology* 37: 1063–1066.

Lee JKW (2009) Using argon as a temporal tracer of large-scale geologic processes. *Chemical Geology* 266: 104–112.

Li J-W, Deng X-D, Zhou M-F, Liu Y-S, Zhao X-F, and Guo J-L (2010) Laser ablation ICP-MS titanite U–Th–Pb dating of hydrothermal ore deposits: A case study of the Tonglushan Cu–Fe–Au skarn deposit, SE Hubei Province, China. *Chemical Geology* 270: 56–67.

Lindgren W (1933) *Mineral Deposits*, 4th ed. New York, London: McGraw-Hill 930 p.

Lindner M, Leich DA, Russ GP, Bazan JM, and Borg RJ (1989) Direct determination of the half-life of ^{187}Re. *Geochimica et Cosmochimica Acta* 53: 1597–1606.

Livne A, Bouchbinder E, Svetlizky I, and Fineberg J (2010) The near-tip fields of fast cracks. *Science* 327: 1359–1363.

Luck J-M and Allègre CJ (1982) The study of molybdenites through the $^{187}Re–^{187}Os$ chronometer. *Earth and Planetary Science Letters* 61: 291–296.

Ludwig KR (2012) *User's Manual for Isoplot 3.75, A Geochronological Toolkit for Microsoft Excel*. Berkeley: Berkeley Geochronology Center Special Publication No. 5 (revised 30 January 2012), p 75.

Ludwig KR and Simmons KR (1992) U–Pb dating of uranium deposits in collapse breccia pipes of the Grand Canyon region. *Economic Geology* 87: 1717–1765.

Ludwig KR, Simmons KR, and Webster JD (1984) U–Pb isotope systematics and apparent ages of uranium ores, Ambrosia Lake and Smith Lake districts, Grants mineral belt, New Mexico. *Economic Geology* 79: 322–337.

Marchesi C, González-Jiménez JM, Gervilla F, et al. (2011) In situ Re–Os isotopic analysis of platinum-group minerals from the Mayarí-Cristal ophiolitic massif (Mayarí-Baracoa ophiolite belt, eastern Cuba): Implications for the origin of Os-isotope heterogeneities in podiform chromitites. *Contributions to Mineralogy and Petrology* 161: 977–990.

Markey RJ, Hannah JL, Morgan JW, and Stein HJ (2003) A double spike for osmium analysis of highly radiogenic samples. *Chemical Geology* 200: 395–406.

Markey R, Stein HJ, Hannah JL, Zimmerman A, Selby D, and Creaser RA (2007) Standardizing Re–Os geochronology: A new molybdenite reference material (Henderson, USA) and the stoichiometry of Os salts. *Chemical Geology* 244: 74–87.

Markey RJ, Stein HJ, and Morgan JW (1998) Highly precise Re–Os dating of molybdenite using alkaline fusion and NTIMS. *Talanta* 45: 935–946.

Martin VM, Davidson J, Morgan D, and Jerram DA (2010) Using the Sr isotope compositions of feldspars and glass to distinguish magma system components and dynamics. *Geology* 38: 539–542.

Massonne H-J, Kennedy A, Nasdala L, and Theye T (2007) Dating of zircon and monazite from diamondiferous quartzofeldspathic rocks of the Saxonian Erzgebirge – Hints at burial and exhumation velocities. *Mineralogical Magazine* 71: 407–425.

Mathez EA and Kent AJR (2007) Variable initial Pb isotopic compositions of rocks associated with the UG2 chromitite, eastern Bushveld Complex. *Geochimica et Cosmochimica Acta* 71: 5514–5527.

Matveev S and Ballhaus C (2002) Role of water in the origin of podiform chromitite deposits. *Earth and Planetary Science Letters* 203: 235–243.

Mauk JL, Hall CM, Chesley JT, and Barra F (2011) Punctuated evolution of a large epithermal province: The Hauraki Goldfield, New Zealand. *Economic Geology* 106: 921–943.

McCandless TE and Ruiz J (1993) Rhenium–osmium evidence for regional mineralization in Southwestern North America. *Science* 261: 1262–1266.

McCandless TE, Ruiz J, and Campbell AR (1993) Rhenium behavior in molybdenite in hypogene and near-surface environments: Implications for Re–Os geochronometry. *Geochimica et Cosmochimica Acta* 57: 889–905.

McFarlane CRM (2006) Palaeoproterozoic evolution of the Challenger Au deposit, South Australia from monazite geochronology. *Journal of Metamorphic Geology* 24: 75–87.

McLeod CL, Davidson JP, Nowell GM, and de Silva S (2012) Disequilibrium melting during crustal anatexis and implications for modeling open magmatic systems. *Geology* 40: 435–438.

Meffre S, Large RR, Scott R, et al. (2008) Age and pyrite Pb-isotope composition of the giant Sukhoi Log sediment-hosted gold deposit, Russia. *Geochimica et Cosmochimica Acta* 72: 2377–2391.

Meyer FM, Kolb J, Sakellaris GA, and Gerdes A (2006) New ages from the Mauritanides Belt: Recognition of Archean IOCG mineralization at Guelb Moghrein, Mauritania. *Terra Nova* 18: 345–352.

Miller CA, Peucker-Ehrenbrink B, Walker BD, and Marcantonio F (2011) Re-assessing the surface cycling of molybdenum and rhenium. *Geochimica et Cosmochimica Acta* 75: 7146–7179.

Monro D (1988) *The Geology and Genesis of the Aitik Copper–Gold Deposit, Arctic Sweden*. Unpublished PhD Thesis, University of Wales, College of Cardiff, UK, p. 386.

Morelli RM, Bell CC, Creaser RA, and Simonetti A (2010) Constraints on the genesis of gold mineralization at the Homestake gold deposit, Black Hills, South Dakota from rhenium–osmium sulfide geochronology. *Mineralium Deposita* 45: 461–480.

Morelli RM, Creaser RA, Selby D, Kelley KD, Leach DL, and King AR (2004) Re–Os sulfide geochronology of the Red Dog sediment-hosted Zn–Pb–Ag deposit, Brooks Range, Alaska. *Economic Geology* 99: 1569–1576.

Morelli RM, Creaser RA, Selby D, Kontak DJ, and Horne RJ (2005) Rhenium–osmium geochronology of arsenopyrite in Meguma Group gold deposits, Meguma terrane, Nova Scotia, Canada: Evidence for multiple gold-mineralizing events. *Economic Geology* 100: 1229–1242.

Morelli R, Creaser RA, Seltmann R, Stuart FM, Selby D, and Graupner T (2007) Age and source constraints for the giant Muruntau gold deposit, Uzbekistan, from coupled Re–Os–He isotopes in arsenopyrite. *Geology* 35: 795–798.

Morgan JW, Stein HJ, Hannah JL, Markey RJ, and Wiszniewska J (2000) Re–Os study of ores from the Suwalki Anorthosite massif, northeast Poland. *Mineralium Deposita* 35: 391–401.

Morgan JW and Walker RJ (1989) Isotopic determination of rhenium and osmium in meteorites using fusion, distillation and ion exchange separations, with resonance ionization mass spectrometry. *Analytica Chimica Acta* 222: 291–300.

Muntean JL, Cline JS, Simon AC, and Longo AA (2011) Magmatic-hydrothermal origin of Nevada's Carlin-type gold deposits. *Nature Geoscience* 4: 122–127.

Nägler TF and Frei R (1997) 'Plug-in' Os distillation. *Schweizerische Mineralogische und Petrographische Mitteilungen (Swiss Bulletin of Mineralogy and Petrology)* 77: 123–127.

Nakai S, Halliday AN, Kesler SE, and Jones HD (1990) Rb–Sr dating of sphalerites from Tennessee and the genesis of Mississippi Valley type ore deposits. *Nature* 346: 354–357.

O'Driscoll B, Day JMD, Daly JS, Walker RM, and McDonough WF (2009) Rhenium–osmium isotopes and platinum-group elements in the Rum layered suite, Scotland: Implications for Cr-spinel seam formation and the composition of the Iceland mantle anomaly. *Earth and Planetary Science Letters* 286: 41–51.

O'Driscoll B, Day JMD, Walker RJ, and Daly JS (2012) Chemical heterogeneity in the upper mantle recorded by peridotites and chromitites from the Shetland ophiolite complex, Scotland. *Earth and Planetary Science Letters* 333–334: 226–237.

Olivo GR, Isnard H, Williams-Jones AE, and Gariépy C (2007) Pb isotope compositions of pyrite from the C quartz–tourmaline vein of the Siscoe gold deposit, Val d'Or, Quebec: Constraints on the origin and age of the gold mineralization. *Economic Geology* 102: 137–146.

Park J-W, Campbell IH, and Eggins SM (2012) Enrichment of Rh, Ru, Ir and Os in Cr spinels from oxidized magmas: Evidence from the Ambae volcano, Vanuatu. *Geochimica et Cosmochimica Acta* 78: 28–50.

Parnell J (1994) Hydrocarbons and other fluids: paragenesis, interactions, and exploration potential inferred from petrographic studies. In: Parnell J (ed.) *Geofluids: Origin, Migration and Evolution of Fluids in Sedimentary Basins*, London: Geological Society Special Publication No. 78: 275–291.

Parnell JS and Swainbank I (1990) Pb-Pb dating of hydrocarbon migration into a bitumen-bearing ore deposit, North Wales. *Geology* 18: 1028–1030.

Paterson SR, Okaya D, Memeti V, Economos R, and Miller RB (2011) Magma addition and flux calculations of incrementally constructed magma chambers in continental margin arcs: Combined field, geochronologic, and thermal modeling studies. *Geosphere* 7: 1439–1468.

Pettke T and Diamond LW (1996) Rb–Sr dating of sphalerite based on fluid inclusion-host mineral isochrons: A clarification of why it works. *Economic Geology* 91: 951–956.

Peucker-Ehrenbrink B and Ravizza G (2000) The marine osmium isotope record. *Terra Nova* 12: 205–219.

Pfaff K, Hildebrandt LH, Leach DL, Jacob DE, and Markl G (2010) Formation of the Wiesloch Mississippi Valley-type Zn–Pb–Ag deposit in the extensional setting of the Upper Rhinegraben, SW Germany. *Mineralium Deposita* 45: 647–666.

Pfaff K, Romer RL, and Markl G (2009) U–Pb ages of ferberite, chalcedony, agate, 'U-mica' and pitchblende: Constraints on the mineralization history of the Schwarzwald ore district. *European Journal of Mineralogy* 21: 817–836.

Poujol M, Boulvais P, and Kosler J (2010) Regional-scale Cretaceous albitization in the Pyrenees: Evidence from in situ U–Th–Pb dating of monazite, titanite, and zircon. *Journal of the Geological Society of London* 167: 751–767.

Rabbia OM, Hernández LB, French DH, King RW, and Ayers JC (2009) The El Teniente porphyry Cu–Mo deposit from a hydrothermal rutile perspective. *Mineralium Deposita* 44: 849–866.

Raith JG and Stein HJ (2006) Variscan ore formation and metamorphism at the Felbertal scheelite deposit (Austria): Constraining tungsten mineralisation from Re–Os dating of molybdenite. *Contributions to Mineralogy and Petrology* 152: 505–521.

Rapp JF, Klemme S, Butler IB, and Harley SL (2010) Extremely high solubility of rutile in chloride and fluoride-bearing metamorphic fluids: An experimental investigation. *Geology* 38: 323–326.

Rasmussen B, Fletcher IR, Muhling JR, Mueller AG, and Hall GC (2007) Bushveld-aged fluid flow, peak metamorphism, and gold mobilization in the Witswatersrand basin, South Africa. *Geology* 35: 931–934.

Rasmussen B, Sheppard S, and Fletcher IR (2006) Testing ore deposit models using in situ U–Pb geochronology of hydrothermal monazite: Paleoproterozoic gold mineralization in northern Australia. *Geology* 34: 77–80.

Ravizza G and Esser BK (1993) A possible link between the seawater osmium isotope record and weathering of ancient sedimentary organic matter. *Chemical Geology* 107: 255–258.

Ravizza G and Turekian KK (1989) Application of the [187]Re–[187]Os system to black shale geochronometry. *Geochimica et Cosmochimica Acta* 53: 3257–3262.

Rempel KU, Williams-Jones AE, and Migdisov AA (2009) The partitioning of molybdenum(VI) between aqueous liquid and vapour at temperatures up to 370°C. *Geochimica et Cosmochimica Acta* 73: 3381–3392.

Rickard DT, Willden M, Mårde Y, and Ryhage R (1975) Hydrocarbons associated with lead–zinc ores at Laisvall, Sweden. *Nature* 255: 131–133.

Ripley EM, Shafer P, Li C, and Hauck SA (2008) Re–Os and O isotopic variations in magnetite from the contact zone of the Duluth complex and the Biwabik iron formation, northeastern Minnesota. *Chemical Geology* 249: 213–226.

Roberts S, Palmer MR, and Waller L (2006) Sm–Nd and REE characteristics of tourmaline and scheelite from the Björkdal gold deposit, northern Sweden: Evidence of an intrusion-related gold deposit? *Economic Geology* 101: 1415–1425.

Romer RL (2001) Lead incorporation during crystal growth and the misinterpretation of geochronological data from low-[238]U/[204]Pb metamorphic minerals. *Terra Nova* 13: 258–263.

Romer RL, Martinsson O, and Perdahl J-A (1994) Geochronology of the Kiruna iron ores and hydrothermal alteration. *Economic Geology* 89: 1249–1261.

Romer RL, Thomas R, Stein HJ, and Rhede D (2007) Dating multiply overprinted Sn-mineralized granites – Examples from the Erzgebirge, Germany. *Mineralium Deposita* 42: 337–359.

Romer RL and Xiao Y (2005) Initial Pb–Sr(–Nd) isotopic heterogeneity in a single allanite–epidote crystal: Implications of reaction history for the dating of minerals with low parent-to-daughter ratios. *Contributions to Mineralogy and Petrology* 148: 662–674.

Rotenberg E, Davis DW, Amelin Y, Ghosh S, and Bergquist BA (2012) Determination of the decay-constant of [87]Rb by laboratory accumulation of [87]Sr. *Geochimica et Cosmochimica Acta* 85: 41–57.

Rubatto D, Müntener O, Barnhoorn A, and Gregory C (2008) Dissolution-reprecipitation of zircon at low-temperature, high-pressure conditions (Lanzo Massif, Italy). *American Mineralogist* 93: 1519–1529.

Schaltegger U (2007) Zircon tiny but timely: Hydrothermal zircons. *Elements* 3(51): 79.

Schaltegger U, Pettke T, Audétat A, Reusser E, and Heinrich C (2005) Magmatic-to-hydrothermal crystallization in the W–Sn mineralized Mole Granite (NSW, Australia) Part I: Crystallization of zircon and REE-phosphates over three million years – A geochemical and U–Pb geochronological study. *Chemical Geology* 220: 215–235.

Schärer U, de Parseval P, Polvé M, and de Saint Blanquat M (1999) Formation of the Trimouns talc-chlorite deposit (Pyrenees) from persistent hydrothermal activity between 112 and 97 Ma. *Terra Nova* 11: 30–37.

Schmitt AK, Grove M, Harrison TM, Lovera O, Hulen J, and Walters M (2003) The Geysers–Cobb Mountain magma system, California (Part 2): Timescales of pluton emplacement and implications for its thermal history. *Geochimica et Cosmochimica Acta* 67: 3443–3458.

Schmitz B, Harper DA, Peucker-Ehrenbrink B, Stouge S, Alwmark C, Cronholm A, Bergstrom SM, Tassinari M, and Wang X (2008) Asteroid breakup linked to the Great Ordovician Biodiversification Event. *Nature Geoscience* 1: 49–53.

Schneider J, Haack U, and Stedingk K (2003) Rb–Sr dating of epithermal vein mineralization stages in the eastern Harz Mountains (Germany) by paleomixing lines. *Geochimica et Cosmochimica Acta* 67: 1803–1819.

Schneider J, Melcher F, and Brauns M (2007) Concordant ages for the giant Kipushi base metal deposit (DR Congo) from direct Rb–Sr and Re–Os dating of sulfides. *Mineralium Deposita* 42: 791–797.

Selby D and Creaser RA (2001) Re–Os geochronology and systematics in molybdenite from the Endako porphyry molybdenum deposit, British Columbia, Canada. *Economic Geology* 96: 197–204.

Selby D and Creaser RA (2004) Macroscale NTIMS and microscale LA-MC-ICP-MS Re–Os isotopic analysis of molybdenite: Testing spatial restrictions for reliable Re–Os age determinations, and implications for the decoupling of Re and Os within molybdenite. *Geochimica et Cosmochimica Acta* 68: 3897–3908.

Selby D, Creaser RA, Dewing K, and Fowler M (2005) Evaluation of bitumen as a [187]Re–[187]Os geochronometer for hydrocarbon maturation and migration: A test case from the Polaris MVT deposit, Canada. *Earth and Planetary Science Letters* 235: 1–15.

Selby D, Creaser RA, Hart CJR, et al. (2002) Absolute timing of sulfide and gold mineralization: A comparison of Re–Os molybdenite and Ar–Ar mica methods from the Tintina Gold Belt, Alaska. *Geology* 30: 791–794.

Selby D, Creaser RA, Stein HJ, Markey RJ, and Hannah JL (2007) Assessment of the [187]Re decay constant by cross calibration of Re–Os molybdenite and U–Pb zircon chronometers in magmatic ore systems. *Geochimica et Cosmochimica Acta* 71: 1999–2013.

Selby D, Kelley KD, Hitzman MW, and Zieg J (2009) Re–Os sulfide (bornite, chalcopyrite, and pyrite) systematics of the carbonate-hosted copper deposits at Ruby Creek, southern Brooks Range, Alaska. *Economic Geology* 104: 437–444.

Shen JJ, Papanastassiou DA, and Wasserburg GJ (1996) Precise Re–Os determinations and systematics of iron meteorites. *Geochimica et Cosmochimica Acta* 60: 2887–2900.

Shi R, Griffin WL, O'Reilly SY, et al. (2012a) Melt/mantle mixing produces podiform chromite deposits in ophiolites: Implications of Re–Os systematics in the Dongqiao Neo-tethyan ophiolite, northern Tibet. *Gondwana Research* 21: 194–206.

Shi G, Li X, Li Q, et al. (2012b) Ion microprobe U–Pb age and Zr-in-rutile thermometry of rutiles from the Daixian rutile deposit in the Hengshan Mountains, Shanxi Province, China. *Economic Geology* 107: 525–535.

Shirey SB and Walker RJ (1995) Carius tube digestion for low-blank rhenium–osmium analysis. *Analytical Chemistry* 67: 2136–2141.

Shirey SB and Walker RJ (1998) The Re–Os isotope system in cosmochemistry and high-temperature geochemistry. *Annual Review of Earth and Planetary Sciences* 26: 423–500.

Sillitoe RH (2010) Porphyry copper systems. *Economic Geology* 105: 3–41.

Sillitoe RH and Mortensen JK (2010) Longevity of porphyry copper formation at Quellaveco, Peru. *Economic Geology* 105: 1157–1162.

Simmons SF and Brown KL (2006) Gold in magmatic–hydrothermal solutions and the rapid formation of a giant ore deposit. *Science* 314: 288–291.

Skirrow RG, Bastrakov EN, Barovich K, et al. (2007) Timing of iron oxide Cu–Au–(U) hydrothermal activity and Nd isotope constraints on metal sources in the Gawler craton, South Australia. *Economic Geology* 102: 1441–1470.

Smoliar MI, Walker RJ, and Morgan JW (1996) Re–Os isotope constraints on the age of Group IIA, IIIA, IVA and IVB iron meteorites. *Science* 271: 1099–1102.

Stacey JS and Kramers JD (1975) Approximation of terrestrial lead isotope evolution by a two-stage model. *Earth and Planetary Science Letters* 26: 207–221.

Stein HJ (2006) Low-rhenium molybdenite by metamorphism in northern Sweden: Recognition, genesis, and global implications. *Lithos* 87: 300–327.

Stein HJ, Barley ME, Zimmerman A, and Cummins B (2007) A 3.3 Ga Mo–Cu porphyry-style deposit at Spinifex Ridge, East Pilbara, Western Australia: Re–Os dating of Paleoarchean molybdenite. *Geochimica et Cosmochimica Acta* 71: A970.

Stein HJ and Bingen B (2002) 1.05–1.01 Ga Sveconorwegian metamorphism and deformation of the supracrustal sequence at Sæsvatn, south Norway: Re–Os dating of Cu–Mo mineral occurrences. In: Blundell D, Neubauer F, and von Quadt A (eds.) *The Timing and Location of Major Ore Deposits in an Evolving Orogen*, London: Geological Society Special Publication No. 204: 319–335.

Stein HJ and Hannah JL (1985) Movement and origin of ore fluids in Climax-type systems. *Geology* 13: 469–474.

Stein HJ, Hannah JL, Zimmerman A, Markey R, Sarkar SC, and Pal AB (2004) A 2.5 Ga porphyry Cu–Mo–Au deposit at Malanjkhand, central India: Implications for Late Archean continental assembly. *Precambrian Research* 134: 189–226.

Stein HJ, Markey RJ, Carriedo J, and Tornos F (2006) Re–Os evidence for the origin of Fe-oxide–(Cu–Au) deposits in SW Iberia at the Frasnian–Famennian boundary. *Geochimica et Cosmochimica Acta* 70: A612.

Stein HJ, Markey RJ, Morgan JW, Du A, and Sun Y (1997) Highly precise and accurate Re–Os ages for molybdenite from the East Qinling molybdenum belt, Shaanxi Province, China. *Economic Geology* 92: 827–835.

Stein HJ, Markey RJ, Morgan JW, Hannah JL, and Scherstén A (2001a) The remarkable Re–Os chronometer in molybdenite: How and why it works. *Terra Nova* 13: 479–486.

Stein HJ, Markey RJ, Morgan JW, et al. (2001b) Re–Os dating of Boddington molybdenites, SW Yilgarn: Two Au mineralization events. *AGSO-Geoscience Australia Record* 2001(37): 469–471.

Stein HJ, Markowiak M, and Mikulski SZ (2005) Metamorphic to magmatic transition captured at the Myszków Mo–W deposit, southern Poland. In: Mao J and Bierlein FP (eds.) *Mineral Deposit Research: Meeting the Global Challenge*, pp. 833–836. Berlin: Springer.

Stein HJ, Morgan JW, Markey RJ, and Hannah JL (1998) An introduction to Re–Os: What's in it for the mineral industry? *SEG Newsletter* 32(1): 8–15.

Stein HJ, Morgan JW, and Scherstén A (2000) Re–Os dating of low-level highly-radiogenic (LLHR) sulfides: The Harnäs gold deposit, southwest Sweden records continental scale tectonic events. *Economic Geology* 95: 1657–1671.

Stein H, Scherstén A, Hannah J, and Markey R (2003) Sub-grain scale decoupling of Re and [187]Os and assessment of laser ablation ICP-MS spot dating in molybdenite. *Geochimica et Cosmochimica Acta* 67: 3673–3686.

Suzuki K, Kagi H, Nara M, Takano B, and Nozaki Y (2000) Experimental alteration of molybdenite: Evaluation of the Re–Os system, infrared spectroscopic profile and polytype. *Geochimica et Cosmochimica Acta* 64: 223–232.

Suzuki K, Qi-Lu, Shimizu H, and Masuda A (1992) Determination of osmium abundance in molybdenite mineral by isotope dilution mass spectrometry with microwave digestion using potassium dichromate as oxidizing agent. *Analyst* 117: 1151–1156.

Suzuki K, Qi-Lu, Shimizu H, and Masuda A (1993) Reliable Re–Os age for molybdenite. *Geochimica et Cosmochimica Acta* 57: 1625–1628.

Suzuki K, Shimizu H, and Masuda A (1996) Re–Os dating of molybdenites from ore deposits in Japan: Implications for closure temperature of Re–Os system for molybdenite and cooling history of molybdenum ore deposits. *Geochimica et Cosmochimica Acta* 60: 3151–3159.

Symons DTA (1994) Paleomagnetism and the Late Jurassic genesis of the Illinois–Kentucky fluorspar deposits. *Economic Geology* 89: 438–449.

Takahashi Y, Tomoya U, Suzuki K, Tanida H, Terada Y, and Hattori KH (2007) An atomic level study of rhenium and radiogenic osmium in molybdenite. *Geochimica et Cosmochimica Acta* 71: 5180–5190.

Terada K, Osaki S, Ishihara S, and Kiba T (1971) Distribution of rhenium in molybdenites from Japan. *Geochemical Journal* 4: 123–141.

Teufel S and Heinrich W (1997) Partial resetting of the U–Pb isotope system in monazite hydrothermal experiments: An SEM and U–Pb isotope study. *Chemical Geology* 137: 273–281.

Tretbar DR, Arehart GB, and Christensen JN (2000) Dating gold deposition in a Carlin-type gold deposit using Rb/Sr methods on the mineral galkhaite. *Geology* 28: 947–950.

Tukey JW (1962) The future of data analysis. *Annals of Mathematical Statistics* 33: 1–67.

Turgeon SC and Creaser RA (2008) Cretaceous oceanic anoxic event 2 triggered by a massive magmatic episode. *Nature* 454: 323–327.

Turner WA, Heaman LM, and Creaser RA (2003) Sm-Nd fluorite dating of Proterozoic low-sulfidation epithermal Au–Ag deposits and U–Pb zircon dating of host rocks at

Mallery Lake, Nunavut, Canada. *Canadian Journal of Earth Sciences* 40: 1789–1804.

Valley PM, Hanchar JM, and Whitehouse MJ (2009) Direct dating of Fe oxide–(Cu–Au) mineralization by U/Pb zircon geochronology. *Geology* 37: 223–226.

Völkening J, Walczyk T, and Heumann KG (1991) Osmium isotope ratio determinations by negative thermal ion mass spectrometry. *International Journal of Mass Spectrometry and Ion Processes* 105: 147–159.

von Quadt A, Erni M, Martinek K, Moll M, Peytcheva I, and Heinrich C (2011) Zircon crystallization and the life-times of ore forming magmatic–hydrothermal system. *Geology* 39: 731–734.

Vonlanthen P, Fitz Gerald JD, Rubatto D, and Hermann J (2012) Recrystallization rims in zircon (Valle d'Arbedo, Switzerland): An integrated cathodoluminescence, LA-ICP-MS, SHRIMP, and TEM study. *American Mineralogist* 97: 369–377.

Walker RJ, Morgan JW, Horan MF, et al. (1994) Re–Os isotopic evidence for an enriched mantle source for the Noril'sk-type ore-bearing intrusions, Siberia. *Geochimica et Cosmochimica Acta* 58: 4179–4197.

Walker RJ, Morgan JW, Smoliar MI, Beary ES, Czamanske GK, and Horan MF (1997) Applications of the ^{190}Pt–^{186}Os isotope system to geochemistry and cosmochemistry. *Geochimica et Cosmochimica Acta* 61: 4799–4807.

Walshaw RD and Menuge JF (1998) Dating of crustal fluid flow by the Rb–Sr isotopic analysis of sphalerite: A review. In: Parnell J (ed.) *Dating and Duration of Fluid Flow and Fluid–Rock Interaction*, vol. 144, pp. 137–143. London: Geological Society Special Publications.

Wanhainen C, Billström K, and Martinsson O (2006) Age, petrology and geochemistry of the porphyritic Aitik intrusion, and its relation to the disseminated Aitik Cu–Au–Ag deposit, northern Sweden. *GFF* 128: 273–286.

Wanhainen C, Billström K, Martinsson O, Stein H, and Nordin R (2005) 160 Ma of magmatic/hydrothermal and metamorphic activity in the Gallivära area: Re–Os dating of molybdenite and U–Pb dating of titanite from the Aitik Cu–Au–Ag deposit, northern Sweden. *Mineralium Deposita* 40: 435–447.

Warner MC (1998) *Geochemical Characterization of Sedimentary Organic Matter and Hydrothermal Petroleum in the Black-Shale-Hosted Zn–Pb Deposit at Red Dog Mine, Western Brooks Range, Alaska*. Unpublished PhD Thesis, Bloomington, Indiana University, p 216.

Watanabe Y and Stein HJ (2000) Re–Os ages for the Erdenet and Tsagaan Suvarga porphyry Cu–Mo deposits, Mongolia, and tectonic implications. *Economic Geology* 95: 1537–1542.

Williams ML, Jercinovic MJ, Harlov DE, Budzyń B, and Heatherington CJ (2011) Resetting monazite ages during fluid-related alteration. *Chemical Geology* 283: 218–225.

Witschard F (1996) Bedrock map 28K Gallivare. 1:50,000. SGU Ai 98–101 (in Swedish).

Witt WK, Stein H, and Cassidy KF (2002) Leonora gold camp: 2.75 Ga gold mineralization overprinted by a 2.66–2.64 Ga orogeny. *Bulletin – Australian Institute of Geoscientists* 36: 237–240.

Xu G, Hannah JL, Stein HJ, et al. (2009) Re–Os geochronology of Arctic black shales to evaluate the Anisian–Ladinian boundary and global faunal correlations. *Earth and Planetary Science Letters* 288: 581–587.

Yang G, Hannah JL, Zimmerman A, Stein HJ, and Bekker A (2009) Re–Os depositional age for Archean carbonaceous slates from the southwestern Superior Province: Challenges and insights. *Earth and Planetary Science Letters* 280: 83–92.

York D, Masliwec A, Kuybida P, et al. (1982) $^{40}Ar/^{39}Ar$ dating of pyrite. *Nature* 300: 52–53.

Yu G, Chen J, Xue C, Chen Y, Chen F, and Du X (2009) Geochronological framework and Pb, Sr isotope geochemistry of the Qingchengzi Pb–Zn–Ag–Au orefield, Northeastern China. *Ore Geology Reviews* 35: 367–382.

Yu G, Yang G, Chen J, Qu W, Du A, and He W (2005) Re–Os dating of gold-bearing arsenopyrite of the Maoling gold deposit, Liaoning province, northeast China and its geological significance. *Chinese Science Bulletin* 50: 1509–1514.

Yuan S, Peng J, Hao S, Li H, Geng J, and Zhang D (2011) *In situ* LA-MC-ICP-MS and ID-TIMS–U–Pb geochronology of cassiterite in the giant Furong tin deposit, Hunan Province, South China: New constraints on the timing of tin-polymetallic mineralization. *Ore Geology Reviews* 43: 235–242.

Zartman RE and Haines SM (1988) The plumbotectonic model for Pb isotopic systematics among major terrestrial reservoirs – A case for bi-directional transport. *Geochimica et Cosmochimica Acta* 52: 1327–1339.

Zheng G, Suzuki K, Miyata Y, and Shimizu H (2012) Osmium concentrations and $^{187}Os/^{188}Os$ ratios of three sediment reference materials. *Geochemical Journal* 46: 143–149.

Zimmerman A, Stein HJ, Hannah JL, Kozelj D, Bogdanov K, and Berza T (2008) Tectonic configuration of the Apusini–Banat–Timok–Srednogorie belt, Balkans–South Carpathians, constrained by high precision Re–Os molybdenite ages. *Mineralium Deposita* 43: 1–21.